

A Mirror Descent-Based Algorithm for Corruption-Tolerant Distributed Gradient Descent

Shuche Wang, *Graduate Student Member, IEEE* and Vincent Y. F. Tan, *Senior Member, IEEE*

Abstract—Distributed gradient descent algorithms have come to the fore in modern machine learning, especially in parallelizing the handling of large datasets that are distributed across several workers. However, scant attention has been paid to analyzing the behavior of distributed gradient descent algorithms in the presence of adversarial corruptions instead of random noise. In this paper, we formulate a novel problem in which adversarial corruptions are present in a distributed learning system. We show how to use ideas from (lazy) mirror descent to design a corruption-tolerant distributed optimization algorithm. Extensive convergence analysis for (strongly) convex loss functions is provided for different choices of the stepsize. We carefully optimize the stepsize schedule to accelerate the convergence of the algorithm, while at the same time amortizing the effect of the corruption over time. Experiments based on linear regression, support vector classification, and softmax classification on the MNIST dataset corroborate our theoretical findings.

Index Terms—Distributed gradient descent, Mirror descent, Adversarial corruptions, Noisy channels, Convergence rates

I. INTRODUCTION

Driven by the growing scale of datasets in various learning tasks, distributed gradient descent has become increasingly important in modern machine learning [2]–[4]. In this paradigm, there is a central parameter server coordinating information among all workers and each worker in the system processes partial gradients using its subset of data [5], [6]. These partial gradients are then collectively used to update the global model parameters. Such a distributed framework not only expedites the learning process but also manages datasets that are too large to be handled in the memory of a single worker or server.

However, there are significant challenges in the use of distributed gradient descent such as the communication overhead [7], the necessity of having resilience against system failures [8], [9], and the presence of adversarial attacks [10]–[13]. In a distributed framework, workers may become unreliable (called *Byzantine* workers in the sequel), which can disrupt the learning process. For instance, as demonstrated in [14], the presence of even a single Byzantine worker can undermine the convergence of a distributed gradient descent algorithm.

In this paper, we consider a new problem concerning the distributed gradient descent algorithm but we take into account

a novel and critical aspect that has, to the best of our knowledge, not been considered before. We consider the presence of adversarial corruptions at each worker in addition to the usual random (Gaussian) noises in the uplink and downlink channels. The corruptions and noises affect the accuracy of partial gradients and parameters. Each worker experiences adversarial corruption, with the total corruption budget being bounded over the entire time horizon. An application of our work could be in a wireless setting with analog transmission of the gradients. However, instead of assuming that this wireless setting is corruption-free, we assume that there are malicious parties in the system that systematically and deterministically modify the gradients that are sent to a central server for downstream machine learning tasks. Our convergence analysis of a modified version of a (lazy) mirror descent-type algorithm addresses the *worst-case* scenario of these corruptions subject to a long-term constraint on the total corruption budget. We show both theoretically and empirically that our algorithm RDGD and its variants such as RDGD-RESTART can be suitably tuned to be corruption tolerant.

A. Main Contributions

Our main contributions are as follows:

- 1) We formulate the problem of distributed gradient descent with adversarial corruptions on the partial gradient vectors held by each of the m workers. We impose a bound $C(T)$ on the total amount of corruptions over the m workers and over the time horizon T . The uplink and downlink channels are also subject to the usual Gaussian noises.
- 2) We design a mirror descent-inspired distributed gradient descent algorithm RDGD that is robust to corruptions. For smooth and convex functions, we show that the expected suboptimality gap of RDGD decays as $O(\frac{1}{\sqrt{T}} + \frac{C(T)}{m\sqrt{T}})$.
- 3) We extend RDGD to the case of loss functions that are strongly convex in addition to being smooth. We bound the suboptimality gap of the enhanced algorithm RDGD-SC. The convergence behavior of RDGD-SC depends on different choices of the stepsize. For a certain choice of stepsize, we observe that the expected suboptimality gap decays as $O(\rho^t + \frac{C(t)}{m})$ where $\rho \in (0, 1)$ is a contraction factor and t is number of iterations, while for another choice, the gap decays as $O(\frac{1}{t^2} + \frac{C(t)}{m\sqrt{t}})$. Thus for the former, there is an exponentially decaying term and a term that does not cause the corruption to vanish; for the latter, there is a (slower) polynomially decaying term and a term that amortizes the corruption.

S. Wang is with the Institute of Operations Research and Analytics, National University of Singapore (Email: shuche.wang@u.nus.edu). V. Y. F. Tan is with the Department of Mathematics, the Department of Electrical and Computer Engineering, and the Institute of Operations Research and Analytics, National University of Singapore (Email: vtan@nus.edu.sg).

This paper was presented in part at the 2024 IEEE International Symposium on Information Theory (ISIT) [1].

This work is funded by a Singapore Ministry of Education AcRF Tier 2 grant (A-8000423-00-00) and two AcRF Tier 1 grants (A-8000980-00-00 and A-8002934-00-00).

- 4) The above observation motivates us to design a *hybrid* algorithm RDGD-RESTART that exploits the benefits of each choice of the stepsize. RDGD-RESTART switches the stepsize schedule at an analytically determined transition time. In RDGD-RESTART, we first exploit the exponential decrease of the suboptimality gap, and eventually amortize the corruption by changing the stepsize.
- 5) The proposed algorithms are assessed numerically through several canonical machine learning models such as linear regression, support vector classification, and softmax classification (on the MNIST dataset). All experimental results corroborate our theoretical findings.

B. Related Works

There are many studies that analyze the effect of *random* corruptions in (stochastic) gradient descent [15]–[17] and its accelerated versions [15], [18], [19]. Our study adopts a distinctly different approach in which we focus on the effect of *malicious adversarial* corruptions, instead of random ones, on distributed gradient descent-type algorithms. In this scenario, some workers send maliciously corrupted gradient information to adversely affect the system's performance. In [20], the authors investigate the robustness of gradient descent in the face of the worst case of corruption, where adversaries can manipulate the corruption up to a certain bounded extent throughout the gradient descent process. In contrast to our *distributed* gradient descent formulation, [20] considers a *centralized* gradient descent scheme. Furthermore, the approach of [20] does not modify the traditional gradient descent algorithm to further mitigate the adversarial corruption's effect.

Another line of research that relevant to our work pertains to *Byzantine distributed gradient descent*. Byzantine faults refer to the scenario where some nodes in the distributed network act arbitrarily or maliciously, potentially leading to incorrect or suboptimal outcomes. One line of solutions is based on the *robust aggregation rules*, including trimmed mean [12], coordinate-wise median [12], geometric median [11], and Krum [14]. However, these robust aggregation rules work under the assumption that the number of Byzantine workers is less than half the total number of workers. Our research approach bifurcates from this line of research since we allow the adversary to *arbitrarily* allocate a bounded amount of corruptions among *all workers*. Our model, however, naturally precludes the possibility of tolerating arbitrary perturbations as median-based approaches that eliminate corruptions of arbitrarily large magnitudes cannot be directly employed.

In addition, these robust aggregation methods can, in general, only recover the parameters obtained from vanilla gradient descent with high probability but not with probability one. To address this challenge, an algorithm called DRACO is presented in [10]. DRACO is a framework that applies *repetition codes* to the computational results of the workers. This requires roughly doubling the replication of each gradient computation, i.e., $2s + 1$ replications of each partial gradient for s malicious workers. Recently, [21] reduced the number of replications from $2s + 1$ to $s + 1$ by introducing an additional step to first *detect* the Byzantine workers. However,

if the channels used for transmitting the parameters are noisy, this idea of replicating each partial gradient does not work perfectly well since the parameter server may fail to reliably select the majority among all the corrupted partial gradients.

The works on adversarial optimization are also closely related to some lines of work in the multi-armed bandit literature, particularly in the adversarial (and not stochastic) setting [22]–[25]. In these settings, adversarial corruption is added to the random rewards, resulting in the agent receiving corrupted versions of the rewards. These approaches typically assume the adversary is capable of arbitrarily allocating corruption in a malicious manner within a total corruption budget. They then use various randomized policies to mitigate the effect of the corruption. However, our study focuses on *distributed gradient descent*, which is a first-order optimization method that is rather different scenarios with bandit feedback.

C. Outline

The rest of this paper is organized as follows. The framework of distributed gradient descent in the presence of adversarial corruptions over noisy channels is presented precisely in Section II. The proposed RDGD algorithm and the analysis of its expected suboptimality gap for smooth loss functions are developed in Section III. In Section IV, we additionally assume the loss function is strongly convex, design an extended algorithm RDGD-SC, and prove a bound on its expected suboptimality gap. The algorithm RDGD-RESTART to mitigate corruption accumulation through a judicious choice of stepsizes is presented in Section V. Numerical experiments are presented in Section VI. Finally, Section VII concludes the paper by suggesting several avenues for further research.

II. PROBLEM SETTING

In this section, we present the framework of distributed gradient descent in the presence of corruptions and noise in channels in both the downlink and the uplink. In addition, we present some basic notations and preliminaries that will facilitate the subsequent analysis.

A. Distributed Gradient Descent

We assume that the samples in a dataset $\mathcal{Z} = \{(x_i, y_i)\}_{i=1}^N$ are drawn from an unknown distribution \mathcal{D} . Here $x_i \in \mathbb{R}^p$ is the i -th feature vector and $y_i \in \mathbb{R}$ is the corresponding scalar response (which could be discrete or continuous). Let $\Theta \subset \mathbb{R}^p$ be the set of model parameters. We seek to minimize the average of loss functions $L : \mathbb{R}^p \times \mathbb{R} \times \Theta \rightarrow \mathbb{R}$ each evaluated over a sample in \mathcal{Z} , i.e., we consider the problem

$$\min_{\theta \in \Theta} \left\{ L(\theta) := \frac{1}{N} \sum_{i=1}^N L(x_i, y_i; \theta) \right\}.$$

In a *centralized* gradient descent scheme, the model parameter $\theta_t \in \Theta$ is updated at iteration t as follows,

$$\theta_{t+1} = \theta_t - \eta_t g_t,$$

where $g_t := \frac{1}{N} \sum_{i=1}^N \nabla L(x_i, y_i; \theta_t)$ is the *full gradient* ($\nabla L(x_i, y_i; \theta)$ is the gradient vector of $L(x_i, y_i; \theta)$ w.r.t. θ) and η_t is an appropriately chosen stepsize at iteration t .

When N is large, it is inefficient to compute the full gradient g_t . Rather, one typically parallelizes the computation of g_t by distributing the data points among $m \ll N$ workers. We assume the N data samples in \mathcal{Z} are uniformly partitioned among the m workers.¹ In particular, the i -th worker maintains a subset \mathcal{Z}_i of the dataset \mathcal{Z} , where $\mathcal{Z}_i \cap \mathcal{Z}_j = \emptyset$, $|\mathcal{Z}_i| = N/m$. Then, worker i computes its *partial gradient vector*

$$g_{i,t} := \frac{1}{|\mathcal{Z}_i|} \sum_{(x,y) \in \mathcal{Z}_i} \nabla L(x,y;\theta_t).$$

This partial gradient vector is then sent to the server.

B. Noisy channel transmission

At the t -th iteration of distributed gradient descent, the parameter server broadcasts the current model parameter $\theta_t \in \Theta$ to all m workers through noisy downlink channels. Worker i receives a noisy version of θ_t as:

$$\theta_{i,t} = \theta_t + v_t^{(i)}, \quad (1)$$

where $v_t^{(i)} = [v_{t,1}^{(i)}, \dots, v_{t,p}^{(i)}]^\top \in \mathbb{R}^p$ is the p -dimensional noise vector at worker i and time t . Furthermore, $v_t^{(i)}$ is a zero-mean random vector consisting of independent and identically distributed (i.i.d.) elements with variance $\mathbb{E}[(v_{t,k}^{(i)})^2] = \sigma_t^2$. Thus,

$$\mathbb{E}[\|v_t^{(i)}\|_2^2] = p\sigma_t^2, \quad \forall i \in [m].$$

Now, the *noisy partial gradient vector* at worker i based on its local dataset \mathcal{Z}_i can be written as

$$g'_{i,t} := \frac{1}{|\mathcal{Z}_i|} \sum_{(x,y) \in \mathcal{Z}_i} \nabla L(x,y;\theta_{i,t}), \quad (2)$$

where $\theta_{i,t}$ is the noisy parameter vector in (1).

C. Corrupted gradients

At iteration t , instead of transmitting the true local gradients, due to Byzantine faults, each worker also suffers an *arbitrary corruption* to its partial gradient vector as follows:

$$\bar{g}_{i,t} = g'_{i,t} + \varepsilon_{i,t}. \quad (3)$$

Here the corruption $\varepsilon_{i,t}$ is a vector in \mathbb{R}^p . Define the ℓ_2 norm of the total corruption at iteration t as:

$$c_t = \left\| \sum_{i=1}^m \varepsilon_{i,t} \right\|_2. \quad (4)$$

This quantifies the aggregate corruption in gradients, introduced by the adversary at iteration t . We denote the corruption vector as $c = [c_1, c_2, \dots, c_T]^\top \in \mathbb{R}^T$ and assume that there is an overall ℓ_2 bound on it across the entire time horizon. The form of the bound we employ is

$$\|c\|_2 = \left(\sum_{t=1}^T c_t^2 \right)^{1/2} \leq C(T). \quad (5)$$

We emphasize that terms $\{\varepsilon_{i,t}\}$ and hence, $\{c_t\}$, and c are *deterministic* quantities induced by Byzantine faults. These

¹Without loss of generality, we assume N is a multiple of m .

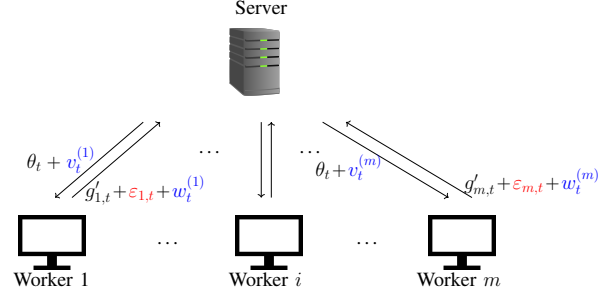


Figure 1. Illustration of the distributed gradient descent setting with corruption over noisy channels. The variables indicated in blue are random Gaussian noises, defined in (1) and (6). The variables indicated in red are deterministic adversarial corruptions specified in (3) and subject to the bound in (5).

are in contrast to the *stochastic noises* in the (downlink and uplink) channels. Our subsequent analysis is thus applicable to the *worst-case* instantiation of these corruptions subject to the constraint in (5).

The i -th worker sends $\bar{g}_{i,t}$ defined in (3) to the parameter server. However, due to the presence of noise in the uplink communication channels, the parameter server receives the following perturbed version of $\bar{g}_{i,t}$ from worker i :

$$\tilde{g}_{i,t} = \bar{g}_{i,t} + w_t^{(i)}, \quad (6)$$

where $w_t^{(i)} = [w_{t,1}^{(i)}, \dots, w_{t,p}^{(i)}]^\top \in \mathbb{R}^p$ is a p -dimensional noise vector at worker i and time t . Furthermore, $w_t^{(i)}$ is a zero-mean random vector consisting of i.i.d. elements with variance $\mathbb{E}[(w_{t,k}^{(i)})^2] = \sigma_t^2$. As a result,

$$\mathbb{E}[\|w_t^{(i)}\|_2^2] = p\sigma_t^2, \quad \forall i \in [m].$$

An illustration of our distributed gradient descent setting with corruptions over noisy channels is presented in Fig. 1.

D. Preliminaries

Consider a continuously differentiable function $f : \Theta \rightarrow \mathbb{R}$, where $\Theta \subseteq \mathbb{R}^p$ is a closed and convex set. The convexity of f is characterized by the following inequality:

$$f(\theta') \geq f(\theta) + \langle \nabla f(\theta), \theta' - \theta \rangle, \quad \forall \theta', \theta \in \Theta.$$

Definition 1 (Smoothness) A differentiable function $f : \Theta \rightarrow \mathbb{R}$ is M -smooth on Θ if for all $\theta, \hat{\theta} \in \Theta$,

$$f(\hat{\theta}) \leq f(\theta) + \langle \nabla f(\theta), \hat{\theta} - \theta \rangle + \frac{M}{2} \|\hat{\theta} - \theta\|_2^2.$$

Definition 2 (Lipschitz Continuity) A function $f : \Theta \rightarrow \mathbb{R}$ is K -Lipschitz continuous on Θ if for all $\theta, \hat{\theta} \in \Theta$,

$$\|f(\hat{\theta}) - f(\theta)\|_2 \leq K \|\hat{\theta} - \theta\|_2.$$

Definition 3 (Strong Convexity) A function $f : \Theta \rightarrow \mathbb{R}$ is μ -strongly convex on Θ if for all $\theta, \hat{\theta} \in \Theta$,

$$f(\hat{\theta}) \geq f(\theta) + \langle \nabla f(\theta), \hat{\theta} - \theta \rangle + \frac{\mu}{2} \|\hat{\theta} - \theta\|_2^2.$$

Definition 4 (Convex Conjugate) The convex conjugate of a function $\psi : \Theta \subset \mathbb{R}^p \rightarrow \mathbb{R}$, denoted as $\psi^* : \mathbb{R}^p \rightarrow \mathbb{R} \cup \{\pm\infty\}$

$$\psi^*(z) = \max_{\theta \in \Theta} \{\langle z, \theta \rangle - \psi(\theta)\}.$$

Algorithm 1 Distributed Gradient Descent Algorithm Robust to Corruptions over Noisy Channels (RDGD)

- 1: **Initialization:** Parameter vector $\theta_0 \in \Theta$, dual vector $z_0 = \nabla\psi(\theta_0)$ for some μ -strongly convex function ψ , algorithm parameters η_t , and T . $\theta_1 = \theta_0$ and $\hat{\theta}_0 = \theta_0$.
 - 2: **for** $t = 1, 2, \dots, T$ **do**
 - 3: **Parameter server:** Send θ_t to all m workers over the downlink noisy channel.
 - 4: **for all** $i \in [m]$ **do in parallel**
 - 5: **Worker i :**
 - 6: Receive $\theta_{i,t} = \theta_t + v_t^{(i)}$ and calculate the corrupted local gradient $g'_{i,t}$ in (2).
 - 7: Send $\tilde{g}_{i,t} = g'_{i,t} + \varepsilon_{i,t}$ to the parameter server via the noisy uplink channel.
 - 8: **end for**
 - 9: **Parameter server:**
 - 10: Receive $\tilde{g}_{i,t} = \tilde{g}_{i,t} + w_t^{(i)}$ for all $i \in [m]$.
 - 11: Compute mean gradient $\tilde{g}_t \leftarrow \frac{1}{m} \sum_{i=1}^m \tilde{g}_{i,t}$
 - 12: Update model parameters:
 - 13: $z_t = z_{t-1} - \eta_t \tilde{g}_t$, i.e., $z_t = -\sum_{k=1}^t \eta_k \tilde{g}_k + z_0$.
 - 14: $\hat{\theta}_t = \frac{H_{t-1}}{H_t} \hat{\theta}_{t-1} + \frac{\eta_t}{H_t} \theta_t$, where $H_t = \sum_{k=1}^t \eta_k$.
 - 15: $\theta_{t+1} = \arg \min_{u \in \Theta} \{ \sum_{k=1}^t \eta_k \langle \tilde{g}_k, u - \theta_k \rangle + D_\psi(u, \theta_0) \}$.
 - 16: **end for**
 - 17: **Output:** The parameter vector $\hat{\theta}_T$.
-

In the following, we assume that whenever we have to compute the convex conjugate ψ^* of a function $\psi : \Theta \rightarrow \mathbb{R}$, this can be done efficiently and potentially in closed form.

The following is a corollary of Danskin's Theorem [26].

Proposition 1 Let $\psi : \Theta \rightarrow \mathbb{R}$ be a differentiable and strongly convex function. Then, the gradient of its convex conjugate ψ^* at any point z is given by:

$$\nabla\psi^*(z) = \arg \max_{\theta \in \Theta} \{ \langle z, \theta \rangle - \psi(\theta) \}.$$

Definition 5 (Bregman Divergence) Let $\psi : \Theta \rightarrow \mathbb{R}$ be a continuously differentiable and strictly convex function called the mirror map. The Bregman divergence $D_\psi : \Theta^2 \rightarrow \mathbb{R}$ is defined as:

$$D_\psi(\theta, \theta') := \psi(\theta) - \psi(\theta') - \langle \nabla\psi(\theta'), \theta - \theta' \rangle.$$

The Bregman divergence $D_\psi(\theta, \theta')$ quantifies the gap between $\psi(\theta)$ and its first-order Taylor approximation at θ' .

III. ROBUST DISTRIBUTED GRADIENT DESCENT TO CORRUPTION OVER NOISY CHANNEL

In this section, we present Robust Distributed Gradient Descent (RDGD), an algorithm that is robust to corruptions over noisy channels. For the minimization of smooth loss functions, the algorithm is described in Algorithm 1. We also provide a bound on the expected suboptimality gap of RDGD.

A. The RDGD Algorithm

At a high level, we utilize a modified lazy mirror descent approach with primal and dual updates. To initialize, we map the initial point θ_0 to $z_0 = \nabla\psi(\theta_0)$ in the dual space via the

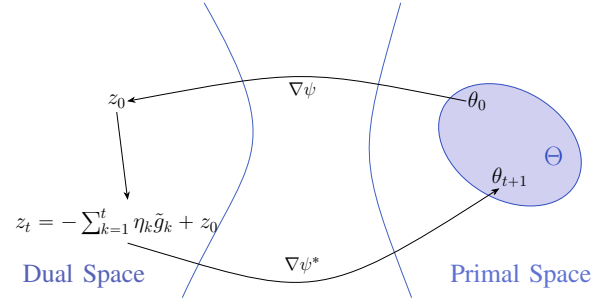


Figure 2. Illustration of primal and dual updates in RDGD.

mirror map $\nabla\psi$ for some suitably chosen μ -strongly convex function ψ . At the t -th iteration of RDGD, the parameter server receives the corrupted partial gradients $\tilde{g}_{i,t}$ for all $i \in [m]$. Then, the parameter server calculates the mean of these $\tilde{g}_{i,t}$ and denotes it as $\tilde{g}_t = \frac{1}{m} \sum_{i=1}^m \tilde{g}_{i,t}$ (Line 11).

Next (Line 13), the server updates z_0 in the dual space to $z_t = z_0 - \sum_{k=1}^t \eta_k \tilde{g}_k$. It then maps z_t back to the point θ_{t+1} in the primal space (Line 15). The illustration of the primal and dual updates in RDGD is presented in Fig. 2. We let

$$\nabla\psi^*(z_t) = \arg \min_{u \in \Theta} \left\{ \sum_{k=1}^t \eta_k \langle \tilde{g}_k, u - \theta_k \rangle + D_\psi(u, \theta_0) \right\}. \quad (7)$$

This process can be considered as a modified version of lazy mirror descent [27]. The intuition behind RDGD is that in (7), we are minimizing an approximation of the loss function, regularized by the Bregman divergence $D_\psi(u, \theta_0)$. The mirror descent procedure operates in a dual space where the effects of corrupted gradients can be modulated differently than if done in the primal space. This reduces the impact of the adversarial corruptions since the updates are not directly in the parameter space where the adversary might have more influence. Regularization makes the optimization process more sensitive to changes in directions that are more likely to be influenced by Byzantine workers, effectively dampening their impact. By shaping the update dynamics through regularization, we limit the influence of corrupted gradients without significantly hindering the convergence speed of legitimate updates.

We denote $\hat{\theta}_t = \frac{H_{t-1}}{H_t} \hat{\theta}_{t-1} + \frac{\eta_t}{H_t} \theta_t$, (where $H_t = \sum_{k=1}^t \eta_k$) as the output at iteration t (Line 14). We note that $\hat{\theta}_t$ is the sum of the weighted gradients based on the history of the gradients. As the analysis shows, this ensures that the final output of RDGD $\hat{\theta}_T$ is robust against noisy updates.

The best choice of the mirror map ψ depends on the specifics of the task. Commonly used mirror maps include:

- 1) ℓ_2 -norm squared $\psi(x) \propto \|x\|_2^2$: Suitable for general optimization due to the balance between computational efficiency and being amenable to deriving convergence guarantees.
- 2) ℓ_1 -norm $\psi(x) = \|x\|_1$: Promotes sparsity in solutions, making it advantageous in high-dimensional settings.
- 3) Negative Entropy $\psi(x) = \sum_i x_i \log x_i$: Effective for tasks involving probability distributions or simplex constraints.

Choosing the appropriate mirror map impacts the algorithm's performance and robustness by tailoring the geometry of the

optimization landscape to the task's requirements. In Section VI-A, we experimentally compare the efficacy of different mirror maps for our specific setting and conclude that the ℓ_2 -norm squared is the most appropriate, at least for the least squares regression task.

B. Convergence Analysis

We apply the approximate duality gap technique proposed in [28] to analyze the convergence of RDGD. We will show how to construct an upper bound G_t of the suboptimality gap $L(\hat{\theta}_t) - L(\theta^*)$, where $\hat{\theta}_t$ is the output of a first-order method at the t -th iteration. Denote $G_t = U_t - L_t$, where $U_t \geq L(\hat{\theta}_t)$ is an upper bound on $L(\hat{\theta}_t)$ and $L_t \leq L(\theta^*)$ is a lower bound on $L(\theta^*)$. Define $H_t := \sum_{k=1}^t \eta_k$. For the lower bound L_t , by the convexity of L , we have

$$L(\theta^*) \geq \frac{\sum_{k=1}^t \eta_k L(\theta_k) + \sum_{k=1}^t \eta_k \langle \nabla L(\theta_k), \theta^* - \theta_k \rangle}{H_t}. \quad (8)$$

To express the gradient $\nabla L(\theta_k)$ in relation to the corrupted gradients $\{\tilde{g}_{i,k} : i \in [m]\}$, we write $\nabla L(\theta_k)$ as $\nabla L(\theta_k) = \tilde{g}_k + \nabla L(\theta_k) - \tilde{g}_k$. Also, by adding and subtracting $\frac{1}{H_t} D_\psi(\theta^*, \theta_0)$ in (8), we have

$$\begin{aligned} H_t L(\theta^*) &\geq \sum_{k=1}^t \eta_k L(\theta_k) + \sum_{k=1}^t \eta_k \langle \tilde{g}_k, \theta^* - \theta_k \rangle \\ &\quad - \sum_{k=1}^t \eta_k \langle \tilde{g}_k - \nabla L(\theta_k), \theta^* - \theta_k \rangle + D_\psi(\theta^*, \theta_0) - D_\psi(\theta^*, \theta_0). \end{aligned}$$

Next, we can obtain our lower bound by replacing θ^* by a minimization over Θ :

$$\begin{aligned} H_t L(\theta^*) &\geq \sum_{k=1}^t \eta_k L(\theta_k) - \sum_{k=1}^t \eta_k \langle \tilde{g}_k - \nabla L(\theta_k), \theta^* - \theta_k \rangle \\ &\quad - D_\psi(\theta^*, \theta_0) + \min_{u \in \Theta} \left\{ \sum_{k=1}^t \eta_k \langle \tilde{g}_k, u - \theta_k \rangle + D_\psi(u, \theta_0) \right\}. \end{aligned}$$

We then define $H_t L_t$ as the lower bound above, i.e.,

$$\begin{aligned} L_t &:= \frac{1}{H_t} \left\{ \sum_{k=1}^t \eta_k L(\theta_k) - \sum_{k=1}^t \eta_k \langle \tilde{g}_k - \nabla L(\theta_k), \theta^* - \theta_k \rangle \right. \\ &\quad \left. - D_\psi(\theta^*, \theta_0) + \min_{u \in \Theta} h_t(u) \right\}, \end{aligned}$$

where

$$h_t(u) := \sum_{k=1}^t \eta_k \langle \tilde{g}_k, u - \theta_k \rangle + D_\psi(u, \theta_0). \quad (9)$$

The promised upper bound is chosen as $U_t = L(\hat{\theta}_t)$, where $\hat{\theta}_t$ is a weighted average of the points $(\theta_k)_{k=1}^t$ generated from RDGD up to t -th iteration (specified in Line 14). Given the forms of U_t and L_t , it is evident that $L(\hat{\theta}_t) - L(\theta^*) \leq G_t$. Therefore, demonstrating the convergence of the algorithm is tantamount to establishing a bound for G_t . We need to track the change of $E_t = H_t G_t - H_{t-1} G_{t-1}$. To facilitate subsequent analyses, we express G_t as:

$$G_t = \frac{H_1}{H_t} G_1 + \frac{\sum_{k=2}^t E_k}{H_t}.$$

According to RDGD, $\theta_{t+1} = \arg \min_{u \in \Theta} h_t(u)$. For our analysis, we first bound $h_t(\theta_{t+1}) - h_{t-1}(\theta_t)$ to track the change of the lower bound L_t in the following lemma. The proof is provided in Appendix A.

Lemma 1 For all $t \geq 2$, the following holds:

$$h_t(\theta_{t+1}) - h_{t-1}(\theta_t) \geq \eta_t \langle \tilde{g}_t, \theta_{t+1} - \theta_t \rangle + D_\psi(\theta_{t+1}, \theta_t).$$

Now, we can derive an upper bound on $H_t G_t - H_{t-1} G_{t-1}$ based on Lemma 1. The proof is provided in Appendix B.

Lemma 2 For all $t \geq 2$, the following holds:

$$\begin{aligned} H_t G_t - H_{t-1} G_{t-1} &\leq \eta_t \langle \tilde{g}_t - \nabla L(\theta_t), \theta^* - \theta_{t+1} \rangle \\ &\quad - \eta_t \langle \nabla L(\theta_t), \theta_{t+1} - \theta_t \rangle - D_\psi(\theta_{t+1}, \theta_t). \end{aligned}$$

Finally, we state the convergence rate of RDGD.

Theorem 1 Let $0 < K, M < \infty$ be such that for all $(x, y) \in \mathbb{R}^p \times \mathbb{R}$, $L(x, y; \cdot)$ are M -smooth and K -Lipschitz continuous. Let $\theta_0 \in \Theta$ be an arbitrary initial point. Let $\{(\theta_t, z_t, \hat{\theta}_t)\}_{t=1}^T$ evolve according to RDGD (Algorithm 1) for some μ -strongly convex function ψ , where $R_\Theta = \max_{\theta \in \Theta} \|\theta - \theta^*\|_2$. Let $\sigma_k \leq \sigma$ for all $k \geq 1$. For a fixed number of iterations T and stepsize $\eta_k = \frac{1}{\sqrt{T}}$, we have for all $k \geq 1$:

$$\begin{aligned} \mathbb{E}[L(\hat{\theta}_T) - L(\theta^*)] &\leq \frac{D_\psi(\theta^*, \theta_0)}{\sqrt{T}} + \frac{K^2}{2\mu} \cdot \frac{1}{\sqrt{T}} \\ &\quad + \frac{R_\Theta C(T)}{m} \cdot \frac{1}{\sqrt{T}} + (M+1)\sqrt{p}\sigma R_\Theta. \end{aligned}$$

The first two terms $\frac{D_\psi(\theta^*, \theta_0)}{\sqrt{T}}$ and $\frac{K^2}{2\mu} \cdot \frac{1}{\sqrt{T}}$ are similar to what one would expect for mirror descent [29]. Since we assume that Θ is bounded, R_Θ is finite. The effect of the adversarial corruption is manifested in the term $\frac{R_\Theta C(T)}{m} \cdot \frac{1}{\sqrt{T}}$, where recall that $C(T)$ (defined in (5)) represents the total corruption among all m workers over T iterations. Even though we do not have a lower bound on the gap $\mathbb{E}[L(\hat{\theta}_T) - L(\theta^*)]$, the scaling $O(\frac{C(T)}{m\sqrt{T}})$ is intuitively order-optimal as, based on (5), if each worker suffers a constant amount of corruption at each time, then $C(T) = \Theta(m\sqrt{T})$. Besides, if the variances of the noises in both downlink and uplink channels are bounded across all iterations (i.e., $\sigma_t^2 \leq \bar{\sigma}^2$ for all t and some $\bar{\sigma}^2 < \infty$), the effect of noisy channels on the bound is $(M+1)\sqrt{p}\sigma R_\Theta$. The proof of Theorem 1 is provided in Appendix C.

If the number of iterations T is not known *a priori*, then η_k cannot depend on T . In this case, we can set $\eta_k = \frac{1}{\sqrt{k}}$ for all $k \geq 1$. A simple corollary of Theorem 1 says that under the same assumptions, for all $t \geq 1$,

$$\begin{aligned} \mathbb{E}[L(\hat{\theta}_t) - L(\theta^*)] &\leq \frac{D_\psi(\theta^*, \theta_0)}{\sqrt{t}} + \frac{K^2}{2\mu} \cdot \frac{\log t}{\sqrt{t}} \\ &\quad + \frac{R_\Theta C(t)}{m} \cdot \sqrt{\frac{\log t}{t}} + (M+1)\sqrt{p}\sigma R_\Theta. \end{aligned}$$

The only difference vis-à-vis the convergence rate specified in Theorem 1 is the corruption term $O(\sqrt{\frac{\log t}{t}})$, which is slightly worse, by a factor of $\sqrt{\log t}$, than its counterpart in Theorem 1. This is due to our incognizance of the number of iterations T .

Algorithm 2 Distributed Gradient Descent Algorithm Robust to Corruptions over Noisy Channels for Strongly-Convex Functions (RDGD-SC)

- 1: **Initialization:** Parameter vector $\theta_0 \in \Theta$, algorithm parameters η_t , dual vector $z_0 = \nabla\psi(\theta_0)$ with $\psi(x) = \frac{\eta_1\alpha}{2}\|x\|_2^2$, $\theta_1 = \theta_0$ and $\hat{\theta}_0 = \theta_0$.
 - 2: **for** $t = 1, 2, \dots$ **do**
 - 3: *Parameter server:* Send θ_t to all the workers over the downlink noisy channel.
 - 4: **for all** $i \in [m]$ **do in parallel**
 - 5: *Worker i :*
 - 6: Receive $\theta_{i,t} = \theta_t + v_t^{(i)}$ and calculate the corrupted local gradient $g'_{i,t}$ in (2).
 - 7: Send $\tilde{g}_{i,t} = g'_{i,t} + \varepsilon_{i,t}$ to parameter server via the noisy uplink channel.
 - 8: **end for**
 - 9: *Parameter server:*
 - 10: Receive $\tilde{g}_{i,t} = \tilde{g}_{i,t} + w_t^{(i)}$, for all $i \in [m]$.
 - 11: Compute mean gradient $\tilde{g}_t \leftarrow \frac{1}{m} \sum_{i=1}^m \tilde{g}_{i,t}$.
 - 12: Update model parameter:
 - 13: $z_t = z_{t-1} - \eta_t \tilde{g}_t$, i.e., $z_t = -\sum_{k=1}^t \eta_k \tilde{g}_k + z_0$.
 - 14: $\hat{\theta}_t = \frac{H_{t-1}}{H_t} \hat{\theta}_{t-1} + \frac{\eta_t}{H_t} \theta_t$, where $H_t = \sum_{k=1}^t \eta_k$.
 - 15: $\theta_{t+1} = \arg \min_{u \in \Theta} \{ \sum_{k=1}^t \eta_k (\langle \tilde{g}_t, u - \theta_k \rangle + \frac{\alpha}{2} \|u - \theta_k\|_2^2) + D_\psi(u, \theta_0) \}$.
 - 16: **end for**
 - 17: **Output:** The sequence of parameter vectors $\{\hat{\theta}_t\}_{t=1}^\infty$.
-

IV. THE STRONGLY CONVEX CASE

In this section, we make a further assumption that the loss function L is strongly convex (in addition to being smooth), and consequently, we are able to improve on the convergence rate in Theorem 1. Our extended algorithm is known as RDGD-SC (Algorithm 2), where the suffix SC stands for Strongly Convex. In essence, assuming that the loss function L is α -strongly convex, the only step that differs from Algorithm 1 is Line 15 therein, which now reads:

$$\theta_{t+1} = \arg \min_{u \in \Theta} \left\{ \sum_{k=1}^t \eta_k \left(\langle \tilde{g}_t, u - \theta_k \rangle + \frac{\alpha}{2} \|u - \theta_k\|_2^2 \right) + D_\psi(u, \theta_0) \right\}. \quad (10)$$

The purpose of the quadratic term $\frac{\alpha}{2} \|u - \theta_k\|_2^2$ in (10) is to exploit the strong convexity of the loss function L to ensure that the expected suboptimality gap decays faster; typically exponentially fast in t .

To analyze the convergence behavior of RDGD-SC, we also apply the approximate duality gap technique used in Section III. For the sake of brevity, we only emphasize the parts that are different from Section III in this section. For the lower bound L_t , exploiting strongly convexity instead of regular convexity, we redefine it as

$$L_t := \frac{1}{H_t} \left\{ \sum_{k=1}^t \eta_k L(\theta_k) - \sum_{k=1}^t \eta_k \langle \tilde{g}_k - \nabla L(\theta_k), \theta^* - \theta_k \rangle - D_\psi(\theta^*, \theta_0) + \min_{u \in \Theta} h_t(u) \right\}$$

where h_t is also redefined as

$$h_t(u) := \sum_{k=1}^t \eta_k \left(\langle \tilde{g}_k, u - \theta_k \rangle + \frac{\alpha}{2} \|u - \theta_k\|_2^2 \right) + D_\psi(u, \theta_0). \quad (11)$$

The template for our analysis is similar to that in the smooth case. The following definitions are identical, starting with $\theta_{t+1} = \arg \min_{u \in \Theta} h_t(u)$ and $G_t = U_t - L_t$. Additionally, we need to track the change of $E_t = H_t G_t - H_{t-1} G_{t-1}$, which leads to $G_t = \frac{H_1}{H_t} G_1 + \frac{\sum_{k=2}^t E_k}{H_t}$. The following lemma bounds $H_1 G_1$ and its proof is provided in Appendix D.

Lemma 3 Let $\psi(x) = \frac{\eta_1\alpha}{2}\|x\|_2^2$, the following holds:

$$H_1 G_1 \leq \frac{\eta_1\alpha}{2} \|\theta^* - \theta_1\|_2^2 + \eta_1 \langle \tilde{g}_1 - \nabla L(\theta_1), \theta^* - \theta_2 \rangle + \frac{\eta_1 K^2}{4\alpha}.$$

The following lemma bounds $h_t(\theta_{t+1}) - h_{t-1}(\theta_t)$ and serves to track the change of the lower bound L_t . Its proof is provided in Appendix E.

Lemma 4 Let $\psi(x) = \frac{\eta_1\alpha}{2}\|x\|_2^2$. For all $t \geq 2$,

$$h_t(\theta_{t+1}) - h_{t-1}(\theta_t) \geq \eta_t \langle \tilde{g}_t, \theta_{t+1} - \theta_t \rangle + \frac{H_t \alpha}{2} \|\theta_{t+1} - \theta_t\|_2^2.$$

Finally, the following lemma whose proof is provided in Appendix F provides a bound of $H_t G_t - H_{t-1} G_{t-1}$.

Lemma 5 Let $\psi(x) = \frac{\eta_1\alpha}{2}\|x\|_2^2$. Then, for all $t \geq 2$,

$$H_t G_t - H_{t-1} G_{t-1} \leq \eta_t \langle \tilde{g}_t - \nabla L(\theta_t), \theta^* - \theta_{t+1} \rangle + \frac{\eta_t K^2}{2\alpha}.$$

Equipped with these preliminary results, the convergence rate of RDGD-SC can be quantified as follows.

Theorem 2 Let $0 < \alpha \leq M < \infty$ and $0 < K < \infty$ be such that for all $(x, y) \in \mathbb{R}^p \times \mathbb{R}$, $L(x, y; \cdot)$ is M -smooth, K -Lipschitz continuous and α -strongly convex. let $\theta_0 \in \Theta$ be an arbitrary initial point. Let $\{(\theta_t, z_t, \hat{\theta}_t)\}_{t=1}^T$ evolve according to RDGD-SC (Algorithm 2) for $\psi(x) = \frac{\eta_1\alpha}{2}\|x\|_2^2$. Let $R_\Theta = \max_{\theta \in \Theta} \|\theta - \theta^*\|_2$ and $\sigma_k \leq \sigma$ for all $k \geq 1$. Let $\eta_1 = 1$ and η_k satisfy $\eta_k \leq \frac{\alpha}{M} H_k$ for all $k \geq 2$. Then for all $t \geq 2$:

$$\begin{aligned} \mathbb{E}[L(\hat{\theta}_t) - L(\theta^*)] &\leq \left(\prod_{k=2}^t \left(1 - \frac{\eta_k}{H_k} \right) \right) \frac{\alpha}{2} \|\theta^* - \theta_0\|_2^2 + \frac{K^2}{2\alpha} \\ &\quad + \frac{R_\Theta C(t)}{m} \cdot \frac{\sqrt{\sum_{k=1}^t \eta_k^2}}{H_t} + (M+1)\sqrt{p}\sigma R_\Theta. \end{aligned} \quad (12)$$

Proof: We write $G_t = \frac{H_1}{H_t} G_1 + \frac{\sum_{k=2}^t E_k}{H_t}$ as

$$\begin{aligned} G_t &= \frac{H_1}{H_2} \frac{H_2}{H_3} \dots \frac{H_{t-1}}{H_t} G_1 + \frac{\sum_{k=2}^t E_k}{H_t} \\ &= \left(1 - \frac{\eta_2}{H_2} \right) \left(1 - \frac{\eta_3}{H_3} \right) \dots \left(1 - \frac{\eta_t}{H_t} \right) G_1 + \frac{\sum_{k=2}^t E_k}{H_t}. \end{aligned}$$

The remaining parts of the proof are essentially the same as those for Theorem 1. ■

Observe that we have the flexibility of setting different stepsize sequences $\{\eta_k\}_{k=1}^\infty$ to achieve different convergence rates in (12). Motivated by this observation, we derive the

following corollary of Theorem 2. The proof is presented in Appendix G.

Corollary 1 (of Theorem 2). For $k \geq 2$, setting

- $\eta_k = \frac{\alpha}{M} H_k$, we have

$$\mathbb{E}[L(\hat{\theta}_t) - L(\theta^*)] \leq \left(1 - \frac{\alpha}{M}\right)^{t-1} \frac{\alpha}{2} \|\theta^* - \theta_0\|_2^2 + \frac{K^2}{2\alpha} + \frac{R_{\Theta} C(t)}{m} + (M+1)\sqrt{p}\sigma R_{\Theta}. \quad (13)$$

- $\eta_k = \frac{2}{k+1} H_k$, we have

$$\mathbb{E}[L(\hat{\theta}_t) - L(\theta^*)] \leq O\left(\frac{\|\theta^* - \theta_0\|_2^2}{t^2} + \frac{1}{\sqrt{t}} \cdot \frac{R_{\Theta} C(t)}{m} + \frac{K^2}{2\alpha} + (M+1)\sqrt{p}\sigma R_{\Theta}\right). \quad (14)$$

If we set $\eta_k = \frac{\alpha}{M} H_k$ (the first case in Corollary 1), we notice that the leading term $\left(1 - \frac{\alpha}{M}\right)^{t-1} \frac{\alpha}{2} \|\theta^* - \theta_0\|_2^2$ resembles the convergence behavior typically observed in the analysis of smooth and strongly convex functions, in scenarios without corruption and noise [30]. This term decays exponentially fast as t grows. However, there is an additional term of the form $\frac{R_{\Theta} C(t)}{m}$ that represents the effect of the corruption and does not vanish with t . Alternatively, if we set $\eta_k = \frac{2}{k+1} H_k$ (the second case of Corollary 1), the leading term vanishes at a slower rate of t^{-2} but the corruption term vanishes at a rate $\frac{C(t)}{m\sqrt{t}}$. This naturally begs the question of whether we can design a “best of both worlds” algorithm to exploit the benefits of both settings of the stepsize η_k to accelerate the overall convergence.

V. CORRUPTION REDUCTION BY EXPLOITING THE BEST OF BOTH WORLDS

Based on the results from Section IV, we observe that for certain natural choices of the stepsize such as $\eta_k = \frac{\alpha}{M} H_k$ with $H_k = \sum_{\ell=1}^k \eta_{\ell}$, the adversarial corruption results in the upper bound on the suboptimality gap in (13) stagnating at a positive, non-vanishing constant. This is clearly undesirable. In this section, we explore how to mitigate this corruption accumulation by proposing an algorithm that switches the stepsize schedule at an appropriate transition time. The main idea is to first exploit the exponential decrease of the expected suboptimality gap by setting $\eta_k = \frac{\alpha}{M} H_k$ until the corruption accumulation begins to dominate the convergence behavior. At this point, we switch to a different stepsize schedule (i.e., $\eta_k = \frac{2}{k+1} H_k$), allowing the corruption to be gradually amortized and thus enabling the hybrid algorithm to further reduce the suboptimality gap as t grows.

In this section, for clarity, we specify the total corruption budget as $C(t) = mt^r$ for some fixed $r \in (0, 1/2)$. We observe from (13) that the suboptimality gap initially decreases and then increases due to the accumulation of the corruption $C(t)$ when we set $\eta_k = \frac{\alpha}{M} H_k$. Hence, we determine the *optimal transition time* t_0 corresponding to the point where the minimum upper bound of suboptimality gap is achieved. The proof of the following lemma is provided in Appendix H.

Algorithm 3 Distributed Gradient Descent Algorithm Robust to Corruptions over Noisy Channels with Restart (RDGD-RESTART)

- 1: **Initialization:** Parameter vector $\theta_0 \in \Theta$, $\eta_1 = 1$, dual vector $z_0 = \nabla \psi(\theta_0)$ with $\psi(x) = \frac{\alpha}{2} \|x\|_2^2$, $\theta_1 = \theta_0$ and $\hat{\theta}_0 = \theta_0$ (defined in (15)).
- 2: **Stage 1:** Run RDGD-SC (Algorithm 2) with $\eta_k = \frac{\alpha}{M} H_k$ from $k \geq 2$. Terminate when $k = t_0$.
- 3: **Stage 2:** Restart RDGD-SC taking θ_{t_0} as the initial point and change the stepsize to $\eta_k = \frac{2}{k+1} H_k$ for all $k \geq t_0 + 1$.
- 4: **Output:** The parameter vector $\hat{\theta}_t$.

Lemma 6 If $\eta_k = \frac{\alpha}{M} H_k$, the minimum of the upper bound of $\mathbb{E}[L(\hat{\theta}_t) - L(\theta^*)]$ in (13) with respect to $t \in \mathbb{N}$ is attained at

$$t_0 = \left\lceil -\frac{(1-r)M}{\alpha} W_{-1}(B(r)) \right\rceil, \quad (15)$$

where $B(r) := -\frac{\alpha}{(1-r)M} \left(\frac{2Mr}{\alpha^2 R_{\Theta} \exp(\alpha/M)} \right)^{\frac{1}{1-r}}$, and W_{-1} denotes the Lambert W function, i.e., the inverse of $f(w) = we^w$.

Note from Lemma 6 that the *transition time* t_0 can be *analytically determined* based on known parameters of the problem such as M , α , and R_{Θ} . Inspired by Lemma 6, we propose the Algorithm 3 that is based on RDGD but with a novel *restart* mechanism (RDGD-RESTART). RDGD-RESTART exploits the exponential decrease in the suboptimality gap until the effect of the accumulation of the corruption starts to dominate the overall bound in (13). To mitigate this, we then switch to a stepsize sequence that decays more slowly to prevent excessive corruption accumulation. This then leads to the bound in (14) dominating the overall convergence behavior subsequently.

We now bound the suboptimality gap $\mathbb{E}[L(\hat{\theta}_t) - L(\theta^*)]$ of RDGD-RESTART. The proof is presented in Appendix I.

Theorem 3 Under the same setting as Theorem 2 and when corruption budget is parameterized as $C(t) = mt^r$ for $r \in (0, 1/2)$, for all $t > t_0$ (defined in (15)), the convergence rate of RDGD-RESTART in Algorithm 3 is:

$$\mathbb{E}[L(\hat{\theta}_t) - L(\theta^*)] \leq \frac{\alpha}{2} \left(1 - \frac{\alpha}{M}\right)^{t_0-1} \frac{t_0(t_0+1)}{t(t_0+1)} \|\theta^* - \theta_0\|_2^2 + R_{\Theta} t^r \cdot A(t, t_0) + \frac{K^2}{2\alpha} + (M+1)\sqrt{p}\sigma R_{\Theta},$$

$$\text{where } A(t, t_0) := \sqrt{\left(\frac{t_0(t_0+1)}{t(t_0+1)}\right)^2 + \left(\frac{2}{t(t_0+1)}\right)^2 \sum_{k=t_0+1}^t k^2}.$$

As $t \rightarrow \infty$, $A(t, t_0)$ decays as $O(1/\sqrt{t})$. We observe from the first term of the bound that in the initial rounds (when $t \leq t_0$), the suboptimality gap decays rapidly due to the exponentially decaying term with contraction factor $1 - \frac{\alpha}{M}$. When $t > t_0$, we observe from the second term that the effect of the corruption is amortized because $r < 1/2$ and $A(t, t_0) = O(1/\sqrt{t})$.

VI. NUMERICAL EXPERIMENTS

In this section, we illustrate the performance of RDGD and its variants through several numerical experiments, including least squares regression and support vector machine (SVM)

classification on synthetically generated datasets, and softmax classification on the MNIST handwritten digits dataset [31]. We compare our proposed algorithms with the vanilla distributed gradient descent (DGD) algorithm, i.e., the parameter vector is simply updated as $\theta_{t+1} = \theta_t - \eta_t \tilde{g}_t$ at the t -th iteration. Note that DGD does not attempt to correct for the presence of corruptions; hence, we expect that it is not robust.

A. Least Squares Regression on Synthetic Datasets

We start with least squares regression on synthetic datasets. The datasets contain $N = 10,000$ data samples. In particular, the loss function of the least-squares regression is as $L(x, y; \theta) = \frac{1}{2}(x^\top \theta - y)^2$ where $\theta \in \mathbb{R}^p$ is the parameter vector with dimensionality $p = 20$. Then, the loss function computed over the entire dataset \mathcal{Z} is $L(\theta) = \frac{1}{2N} \sum_{i=1}^N (x_i^\top \theta - y_i)^2$. We consider one parameter server and $m = 20$ workers.

Each element of the feature vectors x_i is drawn from the standard Gaussian distribution $\mathcal{N}(0, 1)$. We also randomly generate each dimension of the unknown parameter θ^* from $\mathcal{N}(0, 1)$. The scalar responses y_i are obtained by taking the inner product of the feature vectors x_i and the unknown parameter θ^* , followed by adding standard Gaussian noise $\mathcal{N}(0, 1)$. These data samples are then uniformly distributed to all 20 workers. We set the variances of the Gaussian noise in both downlink and uplink channels to $\sigma^2 = 0.5$.

The performance metric is the suboptimality gap $\mathbb{E}[L(\hat{\theta}_t) - L(\theta^*)]$. The results reported are averaged over 100 independent trials. We also report the standard deviations across these 100 experiments. The bound of the total corruption until time t is set to $C(t) = 20t^{0.4}$. As it is difficult to find the worst case corruption pattern, we use the following procedure as a proxy to generate the corruption $\varepsilon_{i,t}$ at each worker $i \in [m]$ and at each time t . In particular, let $\Gamma(\tau) = \sum_{k=1}^\tau c(k)^2$ denote the corruption budget used up to time and including n . Then, the available corruption budget at time t is $\sqrt{C(t)^2 - \Gamma(t-1)}$. Then, we distribute this available corruption budget to each worker randomly. The sign of adversarial corruption at each worker $\text{sign}(\varepsilon_{i,t})$ is set to $-\text{sign}(g'_{i,t})$ for all $i \in [m]$. Also, the stepsize is set to $\eta_t = 1/\sqrt{t}$.

Let $X \in \mathbb{R}^{N \times p}$ be the matrix where each row contains the feature vector x_i^\top . Define $\lambda_{\max}(Q)$ and $\lambda_{\min}(Q)$ as the maximum and minimum eigenvalues of the matrix Q respectively. We run RDGD (Algorithm 1) with the function $\psi(x) = \frac{M}{2} \|x\|_2^2$, where $M = \lambda_{\max}(\frac{1}{N} X^\top X)$. As shown in Fig. 3, our proposed algorithm achieves a significantly smaller suboptimality gap more quickly and consistently compared to the traditional DGD algorithm.

Since the effectiveness of the mirror descent procedure relies on the choice of the mirror map ψ , we conducted additional experiments to evaluate the performance of mirror descent under ψ 's. Specifically, we considered the negative entropy and the ℓ_1 -norm as mirror maps, in addition to the ℓ_2 -norm squared used in the preceding experiments. The results, presented in Fig. 4, demonstrate that the quadratic mirror map is the most suitable for least squares regression.

Next, we verify the efficacy of the restart mechanism RDGD-RESTART (in Algorithm 3) when the loss function is

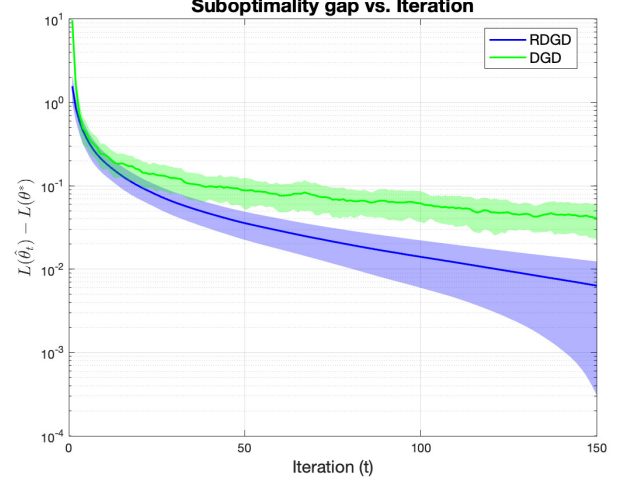


Figure 3. Performances of RDGD and DGD for least squares regression

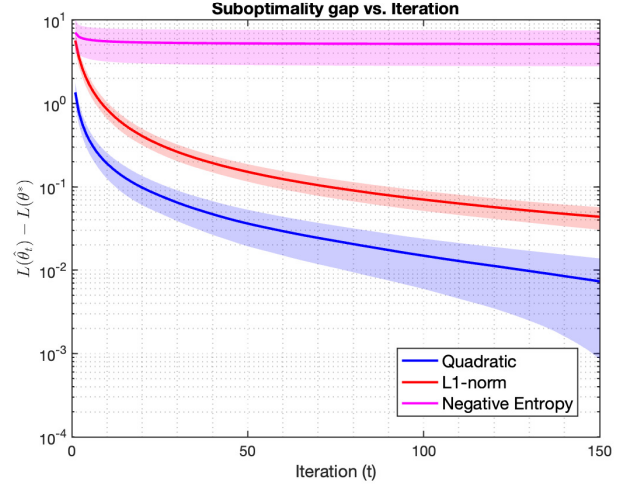


Figure 4. Performances of different mirror maps ψ for least squares regression

smooth and strongly convex. In particular, we modify the loss function of least-squares regression by adding an ℓ_2 -squared regularization term, i.e., $L(x, y; \theta) = \frac{1}{2}(x^\top \theta - y)^2 + \frac{\lambda}{2} \|\theta\|_2^2$, where we set $\lambda = 0.01$. Now, we run RDGD-RESTART for this strongly convex loss function. We set the strongly convex parameter as $\alpha = \lambda_{\min}(\frac{1}{N} X^\top X + \lambda \mathbf{I}_p)$ and the smooth parameter as $M = \lambda_{\max}(\frac{1}{N} X^\top X + \lambda \mathbf{I}_p)$ respectively. The variance of the Gaussian noises in the uplink and downlink is set to $\sigma^2 = 0.1$. The function $\psi(x) = \frac{\alpha}{2} \|x\|_2^2$.

As shown in Fig. 5, if one chooses the stepsize sequence $\eta_k = \frac{\alpha}{M} H_k$, the adversarial corruption accumulates after a certain point, resulting in a stagnation of the suboptimality gap. However, it is also worth noting that the gap decreases much more rapidly when $\eta_k = \frac{\alpha}{M} H_k$ compared to when $\eta_k = \frac{2}{k+1} H_k$ initially. In our proposed algorithm with a restart mechanism RDGD-RESTART, the gap decreases rapidly until a transition time t_0 which can be determined analytically.

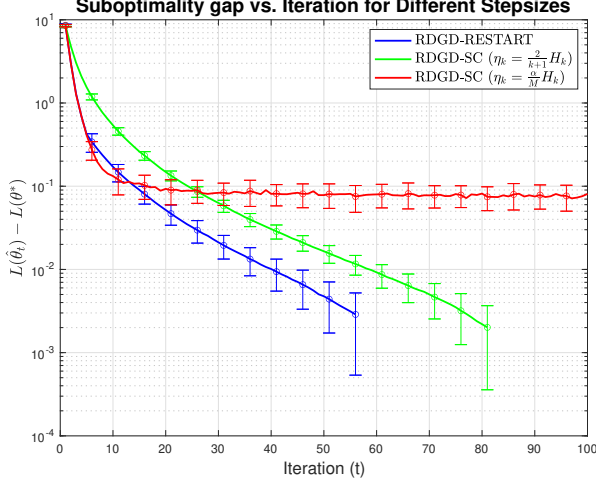


Figure 5. Comparison of the performances of RDGD-SC with different stepsizes $\{\eta_k\}$ to RDGD-RESTART

After time $t_0 + 1$, we switch the stepsize sequence from $\eta_k = \frac{\alpha}{M} H_k$ to $\eta_k = \frac{2}{k+1} H_k$. As can be seen, the gap subsequently decreases with t . Our proposed algorithm RDGD-RESTART converges faster than the $\eta_k = \frac{2}{k+1} H_k$ case throughout the entire process, indicating a smaller time complexity to achieve the same suboptimality gap. The experimental results presented in Fig. 5 thus corroborate our theoretical analysis in Section V. Hence, our proposed algorithm with a restart mechanism RDGD-RESTART successfully takes advantage of the exponential decrease in the gap until corruption accumulation occurs, then mitigates the adverse effects of the accumulation by switching to another stepsize sequence.

B. Classification using L2 Support Vector Machines

Next we verify the efficacy of RDGD on a binary classification task with a loss function that is different from that used in the previous section. Specifically, we consider L2-SVM² [32], [33] and we use the accuracy of the binary classification task as our performance metric. The label y_i is generated such that it takes values from the set $\{1, -1\}$ with equal probability. For each y_i , the corresponding feature vector x_i is generated from a multivariate normal distribution. If $y_i = 1$, x_i is drawn from $\mathcal{N}(\mu, \gamma \mathbf{I}_p)$, and if $y_i = -1$, x_i is drawn from $\mathcal{N}(-\mu, \gamma \mathbf{I}_p)$, where μ is the vector of all ones of length p and $\gamma = 4$.

We generated $N = 10,000$ data samples which are then split into 8,000 samples for training and 2,000 samples for testing. The primal objective function used in L2-SVM is $L(x, y; \theta) = \max\{0, 1 - y(x^\top \theta)\}^2 + \frac{\lambda}{2} \|\theta\|_2^2$, where λ is set to 0.1. We compare RDGD with vanilla DGD under varying levels of corruption budgets $C(T)$, with a fixed noise variance $\sigma^2 = 1$ in the (uplink and downlink) communication channels. Specifically, the total corruption bound up to time T is set as $C(T) = 20T^r$, where $r \in \{0.25, 0.3, 0.35\}$. The total

²We consider L2-SVM instead of the usual L1-SVM since the loss function is smooth for the former.

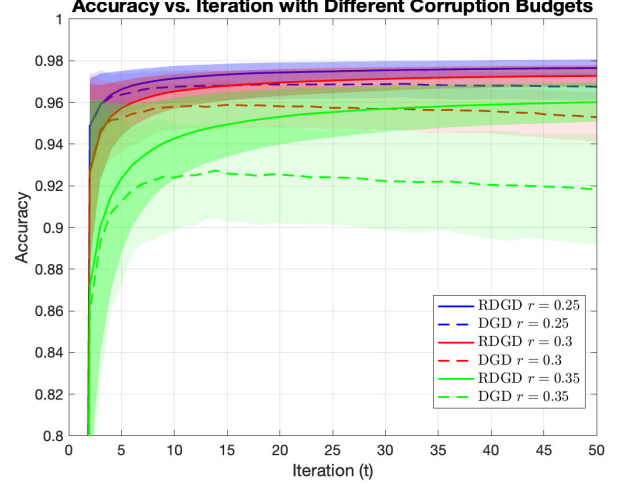


Figure 6. RDGD for L2-SVM classification

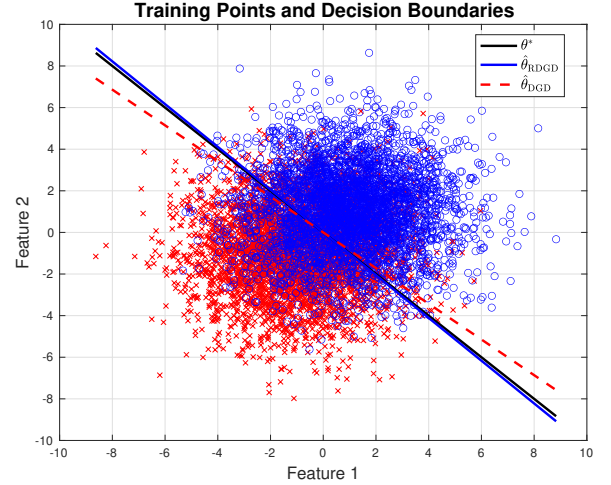


Figure 7. Decision Boundaries for L2-SVM classification

corruption budget is uniformly allocated to each iteration and worker, i.e., $c(t) = C(T)/\sqrt{T}$, for all $t \in [T]$.

As shown in Fig. 6, RDGD converges rapidly and achieves high accuracy at any level of the corruption budget. However, the accuracy of the classification of the vanilla DGD algorithm is lower than RDGD and is highly sensitive to the level of the corruption budget. DGD fails when the corruption budget exceeds a certain level (e.g., $r = 0.35$). In Fig. 7, we display the decision boundaries for the first two dimensions of the parameter vectors $\hat{\theta}_{RDGD}$ and $\hat{\theta}_{DGD}$ obtained by RDGD and DGD respectively when $r = 0.35$. Note that $\hat{\theta}_{RDGD}$ is almost identical to θ^* . However, $\hat{\theta}_{DGD}$ deviates significantly from θ^* , showing that DGD is not robust.

C. Softmax Classification on the MNIST Dataset

In our final set of experiments, we consider a multi-class classification task on the classical MNIST dataset, which

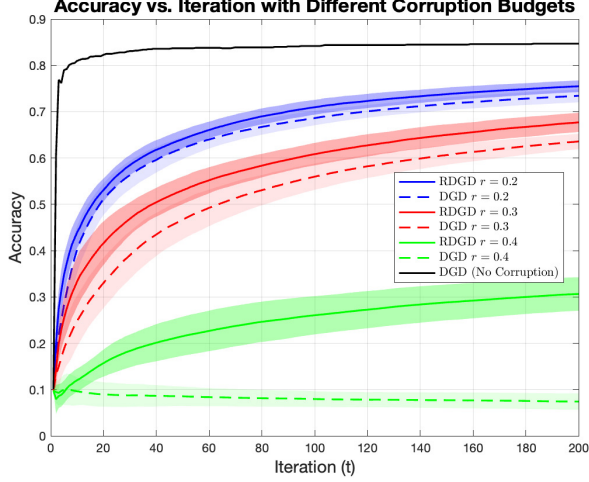


Figure 8. RDGD for the MNIST dataset with different levels of corruption

contains 10 classes (i.e., the number of values that each label y_i can take on is 10), 60,000 training samples and 10,000 test samples. The performance metric is the classification accuracy on the test samples. The dimensionality p of the data points is $784 = 28 \times 28$ and the number of workers m is set to 20. We use the *cross-entropy loss* to optimize the *softmax classifier*.

1) *Performance under a bounded amount of adversarial corruptions:* In Fig. 8, we compare RDGD with vanilla DGD under varying levels of corruption budgets $C(T)$, with a fixed noise variance $\sigma^2 = 0.5$ in the channels. Specifically, the total corruption bound up to time T is set as $C(T) = 100T^r$, where $r \in \{0.2, 0.3, 0.4\}$. The total corruption budget is also uniformly allocated to each iteration and each worker as in the previous subsection. As shown in Fig. 8, RDGD outperforms the traditional DGD algorithm across all levels of the corruption budget. Furthermore, we observe that RDGD achieves higher accuracy as the value of r and hence, the amount of corruption, decreases. The vanilla DGD algorithm reduces to random guessing (success rate $\approx 10\%$) when the corruption budget exceeds a certain level (i.e., $r = 0.4$).

To further evaluate the performance of RDGD, we conducted experiments comparing it against three baseline algorithms: the traditional DGD algorithm, Trimmed Mean by Yin *et al.* [12], and Krum by Blanchard *et al.* [14]. The total corruption bound up to time T and the fraction of Byzantine workers are set to be $C(T) = 150T^{0.3}$ and 0.3 respectively. Note that the baseline algorithms (Trimmed Mean and Krum) are only applicable when the fraction of Byzantine workers is less than half, whereas RDGD can handle an arbitrary proportion. The total corruption budget is *uniformly allocated* to each iteration and each Byzantine worker. The results, shown in Fig. 9, indicate that RDGD consistently outperformed the baseline methods over all iterations. RDGD achieved a faster convergence rate and accuracy compared to DGD, Trimmed Mean, and Krum.

2) *Performance under adversarial corruption in the final iterations:* As mentioned, it is difficult to find the worst

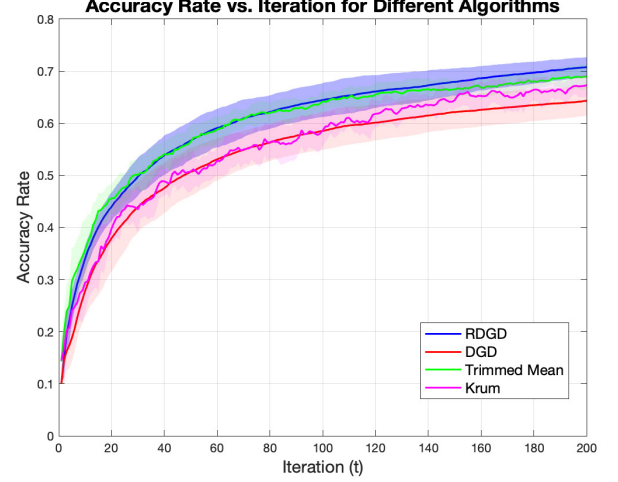


Figure 9. Accuracy rates of different algorithms for the MNIST dataset with adversarial corruption

case corruption pattern. In addition to allocating the available corruption budget to each iteration and each Byzantine worker uniformly, we also evaluate the performance of RDGD and the baselines when the corruption is only allocated to *the last 20% of iterations*; this is particularly challenging for all algorithms as they have to suddenly adapt to the presence of the corruptions towards the end of the horizon. The total corruption bound up to time T and the fraction of Byzantine workers are set to $C(T) = 150T^{0.3}$ and 0.3 respectively. Fig. 10 illustrates the performance of different algorithms when the corruption is introduced only during the last 20% of the iterations (i.e., from 161 to 200). In the first 160 iterations, when no corruption is present, all algorithms exhibit steady increases in accuracy, with RDGD demonstrating the fastest convergence and the highest accuracy. However, in the last 20% of the iterations, the malicious gradients degrade the performance of the baselines, causing noticeable drops in their accuracy, whereas RDGD maintains its robustness.

3) *Performance under periodic adversarial corruption:* To further show it is difficult to find the worst-case corruption pattern, we consider periodic adversarial corruptions, where the corruption is introduced at the $[50, 100, 150, 200]$ -th iterations. The total corruption bound up to time T and the fraction of Byzantine workers are set to $C(T) = 150T^{0.3}$ and 0.3 respectively. Hence, the corruption level at these 4 iterations is large given that we keep the corruption level the same at $C(T) = 150T^{0.3}$. The sign of adversarial corruption at each Byzantine worker $\text{sign}(\varepsilon_{i,t})$ is set to be $-\text{sign}(\tilde{g}_{i,t})$. Then we add the corruption vector $\varepsilon_{i,t}$ to $g'_{i,t}$, and obtain $\bar{g}_{i,t} = g'_{i,t} + \varepsilon_{i,t}$. We checked the signs of each of the dimensions of $\bar{g}_t \in \mathbb{R}^p$ and notice that for each Byzantine worker, more than 90% of the dimensions of \bar{g}_t have their signs flipped. This shows that the corruption added significantly alters the direction of the gradient vector \bar{g}_t , implying that its effect is substantial. As shown in Fig. 11, DGD exhibits a distinctive “sawtooth” pattern, sharp periodic drops in accuracy, followed by gradual

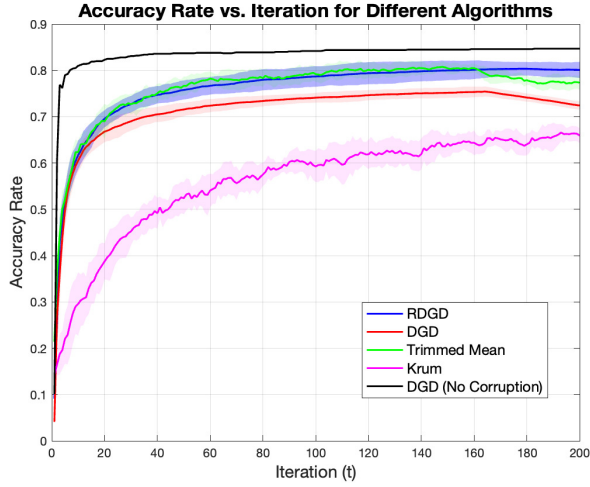


Figure 10. Accuracy rates for different algorithms for the MNIST dataset with allocating corruptions to last 20% of iterations

recovery. These periodic drops occur when corruptions are introduced, demonstrating DGD’s vulnerability to “sudden” Byzantine attacks. Meanwhile, the performance of RDGD remains high throughout the whole process. This experiment again demonstrates RDGD’s robustness.

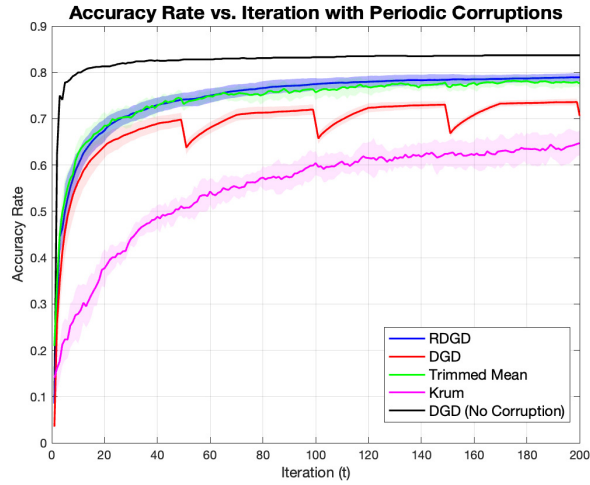


Figure 11. Accuracy rates for different algorithms for the MNIST dataset with periodic corruption

4) *Performance under “A Little Is Enough” attack:* Besides adversarial corruption with a fixed budget, we also evaluate RDGD for the “A Little Is Enough” (ALIE) attack proposed by Baruch *et al.* [34], which is designed to destroy robust aggregation methods such as Trimmed Mean and Krum. We denote the set of Byzantine workers as \mathcal{B} . ALIE attacks the gradients at the Byzantine worker $i \in \mathcal{B}$ by setting their updates to be $g_{i,t} = \mu_t + z \cdot \sigma_t$, where μ_t and σ_t are respectively the mean and standard deviation of the gradients at iteration t among all the m workers, and z is an attack intensity pa-

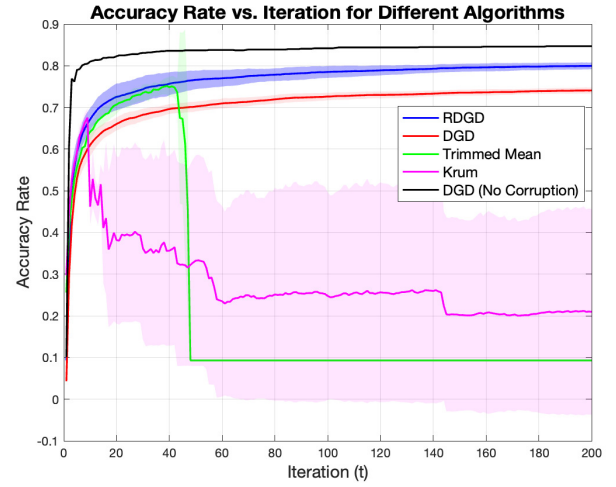


Figure 12. Accuracy rates for different algorithms for the MNIST dataset with ALIE attack

parameter. This allows adversarial updates to remain statistically plausible, making them extremely difficult to detect. We set $z = 1.5$ and the fraction of Byzantine workers to be 0.3.

As shown in Fig. 12, RDGD exhibited remarkable robustness against this attack, achieving a consistently accuracies. In contrast, baseline methods such as Trimmed Mean and Krum showed significant drops in accuracy after the early iterations.

VII. CONCLUSION

In this paper, we considered a robustification of the standard distributed gradient descent algorithm used extensively in the parallelization of massive datasets in the modern era. In addition to standard channel noises on the uplink and downlink of the communication channels, we also considered mitigating the effects of *adversarial corruptions* at the workers via a mirror descent-type algorithm RDGD and its strongly convex extension RDGD-SC. Different convergence rates of the suboptimality gap were obtained by setting different stepsizes in RDGD-SC. We also provided a theoretical analysis of a unified algorithm RDGD-RESTART that attains the “best-of-both-worlds” with regard to the choice of the different stepsizes in RDGD-SC. Extensive numerical experiments show that (i) RDGD performs much better, in terms of the suboptimality gap and classification accuracy, than standard DGD in reducing the effect of the corruption and (ii) the restarting mechanism in RDGD-RESTART is effective in speeding up the overall convergence rate for strongly convex loss functions.

We may consider the following avenues for future research. First, to model the scenario in which *some*, but not all, workers are compromised, we may redefine c_t in (4) as $c_t = \sum_{i=1}^m \|\varepsilon_{i,t}\|_2$. This encourages sparsity among the $\varepsilon_{i,t}$ ’s for fixed t . Second, we may derive information-theoretic *lower bounds* on the suboptimality gap as a function of the corruption $C(T)$ to determine the tightness of the upper bounds.

APPENDIX A
PROOF OF LEMMA 1

Proof: By the definition of h_t in (9), we have $h_t(\theta_{t+1}) - h_{t-1}(\theta_{t+1}) \geq \eta_t \langle \tilde{g}_t, \theta_{t+1} - \theta_t \rangle$.

Then, based on the definition of the Bregman divergence, we have $h_{t-1}(\theta_{t+1}) - h_{t-1}(\theta_t) = \langle \nabla h_{t-1}(\theta_t), \theta_{t+1} - \theta_t \rangle + D_{h_{t-1}}(\theta_{t+1}, \theta_t)$ and $D_{h_{t-1}}(\theta_{t+1}, \theta_t) = D_\psi(\theta_{t+1}, \theta_t)$. However, since $\theta_t = \operatorname{argmin}_{u \in \Theta} h_{t-1}(u)$, we have $\langle \nabla h_{t-1}(\theta_t), \theta_{t+1} - \theta_t \rangle \geq 0$. Thus,

$$h_t(\theta_{t+1}) - h_{t-1}(\theta_t) \geq \eta_t \langle \tilde{g}_t, \theta_{t+1} - \theta_t \rangle + D_\psi(\theta_{t+1}, \theta_t)$$

as desired. ■

APPENDIX B
PROOF OF LEMMA 2

Proof: Based on Lemma 1, we have:

$$\begin{aligned} H_t L_t - H_{t-1} L_{t-1} &\geq \eta_t L(\theta_t) - \eta_t \langle \tilde{g}_t - \nabla L(\theta_t), \theta^* - \theta_t \rangle \\ &\quad + \eta_t \langle \tilde{g}_t, \theta_{t+1} - \theta_t \rangle + D_\psi(\theta_{t+1}, \theta_t) \\ &= \eta_t L(\theta_t) - \eta_t \langle \tilde{g}_t - \nabla L(\theta_t), \theta^* - \theta_{t+1} \rangle \\ &\quad + \eta_t \langle \nabla L(\theta_t), \theta_{t+1} - \theta_t \rangle + D_\psi(\theta_{t+1}, \theta_t). \end{aligned}$$

Then, it follows that:

$$\begin{aligned} H_t G_t - H_{t-1} G_{t-1} &\leq H_t L(\hat{\theta}_t) - H_{t-1} L(\hat{\theta}_{t-1}) - \eta_t L(\theta_t) \\ &\quad + \eta_t \langle \tilde{g}_t - \nabla L(\theta_t), \theta^* - \theta_{t+1} \rangle - \eta_t \langle \nabla L(\theta_t), \theta_{t+1} - \theta_t \rangle \\ &\quad - D_\psi(\theta_{t+1}, \theta_t). \end{aligned}$$

From RDGD in Algorithm 1 and the convexity of L , we can write $H_t L(\hat{\theta}_t) - H_{t-1} L(\hat{\theta}_{t-1}) - \eta_t L(\theta_t)$ as:

$$\begin{aligned} &\eta_t L(\hat{\theta}_t) + H_{t-1} (L(\hat{\theta}_t) - L(\hat{\theta}_{t-1})) - \eta_t L(\theta_t) \\ &\leq \eta_t (L(\hat{\theta}_t) - L(\theta_t)) + H_{t-1} \langle \nabla L(\hat{\theta}_t), \hat{\theta}_t - \hat{\theta}_{t-1} \rangle \\ &= \eta_t (L(\hat{\theta}_t) - L(\theta_t)) - \eta_t \langle \nabla L(\hat{\theta}_t), \hat{\theta}_t - \theta_t \rangle \\ &\leq \eta_t \langle \nabla L(\hat{\theta}_t), \hat{\theta}_t - \theta_t \rangle - \eta_t \langle \nabla L(\hat{\theta}_t), \hat{\theta}_t - \theta_t \rangle \\ &= 0. \end{aligned} \tag{16}$$

Hence, we conclude that

$$\begin{aligned} H_t G_t - H_{t-1} G_{t-1} &\leq \eta_t \langle \tilde{g}_t - \nabla L(\theta_t), \theta^* - \theta_{t+1} \rangle \\ &\quad - \eta_t \langle \nabla L(\theta_t), \theta_{t+1} - \theta_t \rangle - D_\psi(\theta_{t+1}, \theta_t) \end{aligned}$$

as desired. ■

APPENDIX C
PROOF OF THEOREM 1

Proof: Based on Lemma 2, we have

$$\begin{aligned} H_t G_t - H_{t-1} G_{t-1} &\leq \eta_t \langle \tilde{g}_t - \nabla L(\theta_t), \theta^* - \theta_{t+1} \rangle \\ &\quad - \eta_t \langle \nabla L(\theta_t), \theta_{t+1} - \theta_t \rangle - D_\psi(\theta_{t+1}, \theta_t). \end{aligned}$$

By the definition of the Bregman divergence and the μ -strong convexity of the mirror map ψ , we have $D_\psi(\theta_{t+1}, \theta_t) \geq \frac{\mu}{2} \|\theta_{t+1} - \theta_t\|_2^2$. Hence,

$$\begin{aligned} &-\eta_t \langle \nabla L(\theta_t), \theta_{t+1} - \theta_t \rangle - D_\psi(\theta_{t+1}, \theta_t) \\ &\leq \eta_t K \|\theta_{t+1} - \theta_t\|_2 - \frac{\mu}{2} \|\theta_{t+1} - \theta_t\|_2^2 \leq \frac{\eta_t^2 K^2}{2\mu}, \end{aligned}$$

where the first inequality follows from the Cauchy-Schwarz inequality and the fact that a differentiable K -Lipschitz continuous and convex function $L(\cdot)$ has a gradient vector $\nabla L(\cdot)$ with norm bounded by K [35, Lemma 2.6], and the second inequality follows from the fact that $2ab - b^2 \leq a^2$.

Recall that $g_{i,k} = \frac{1}{|\mathcal{Z}_i|} \sum_{(x,y) \in \mathcal{Z}_i} \nabla L(x,y; \theta_k)$. Hence, we can write $\nabla L(\theta_k) = \frac{1}{m} \sum_{i=1}^m g_{i,k}$ and

$$\begin{aligned} &\langle \tilde{g}_k - \nabla L(\theta_k), \theta^* - \theta_{k+1} \rangle \\ &= \left\langle \frac{1}{m} \left(\sum_{i=1}^m g'_{i,k} + \sum_{i=1}^m \varepsilon_{i,k} + \sum_{i=1}^m w_k^{(i)} \right) - \frac{1}{m} \sum_{i=1}^m g_{i,k}, \theta^* - \theta_{k+1} \right\rangle \\ &= \frac{1}{m} \left\langle \sum_{i=1}^m g'_{i,k} - \sum_{i=1}^m g_{i,k}, \theta^* - \theta_{k+1} \right\rangle + \frac{1}{m} \left\langle \sum_{i=1}^m \varepsilon_{i,k}, \theta^* - \theta_{k+1} \right\rangle \\ &\quad + \frac{1}{m} \left\langle \sum_{i=1}^m w_k^{(i)}, \theta^* - \theta_{k+1} \right\rangle. \end{aligned}$$

Recall that $R_\Theta = \max_{\theta \in \Theta} \|\theta - \theta^*\|_2$. It follows that

$$\begin{aligned} &\langle \tilde{g}_k - \nabla L(\theta_k), \theta^* - \theta_{k+1} \rangle \\ &\leq \frac{MR_\Theta}{m} \sum_{i=1}^m \|v_k^{(i)}\|_2 + \frac{c_k R_\Theta}{m} + \frac{R_\Theta}{m} \sum_{i=1}^m \|w_k^{(i)}\|_2. \end{aligned}$$

Then, we have

$$\begin{aligned} &\sum_{k=1}^t \eta_k \langle \tilde{g}_k - \nabla L(\theta_k), \theta^* - \theta_{k+1} \rangle \\ &\leq \frac{R_\Theta}{m} \sum_{k=1}^t \eta_k c_k + \frac{MR_\Theta}{m} \sum_{k=1}^t \eta_k \sum_{i=1}^m \|v_k^{(i)}\|_2 \\ &\quad + \frac{R_\Theta}{m} \sum_{k=1}^t \eta_k \sum_{i=1}^m \|w_k^{(i)}\|_2. \end{aligned} \tag{17}$$

Taking the expectation on both sides of (17) and assuming $\sigma_k^2 \leq \sigma^2$ for all $k \geq 1$, we obtain

$$\begin{aligned} &\mathbb{E} \left[\sum_{k=1}^t \eta_k \langle \tilde{g}_k - \nabla L(\theta_k), \theta^* - \theta_{k+1} \rangle \right] \\ &\leq \frac{R_\Theta}{m} \langle \boldsymbol{\eta}_t, \mathbf{c}_t \rangle + (M+1) \sqrt{p} \sigma R_\Theta \sum_{k=1}^t \eta_k, \end{aligned}$$

where $\boldsymbol{\eta}_t = [\eta_1, \dots, \eta_t]^\top$ and $\mathbf{c}_t = [c_1, \dots, c_t]^\top$.

Since the overall bound on the total corruption up to and including time t is $C(t)$ such that $\sqrt{\sum_{k=1}^t c_k^2} \leq C(t)$, by the Cauchy-Schwarz inequality, we have

$$\begin{aligned} &\mathbb{E} \left[\sum_{k=1}^t \eta_k \langle \tilde{g}_k - \nabla L(\theta_k), \theta^* - \theta_{k+1} \rangle \right] \\ &\leq \frac{R_\Theta C(t)}{m} \sqrt{\sum_{k=1}^t \eta_k^2} + (M+1) \sqrt{p} \sigma R_\Theta H_t. \end{aligned} \tag{18}$$

Next, we bound $H_1 G_1$ as follows:

$$\begin{aligned} H_1 G_1 &= H_1 U_1 - H_1 L_1 \\ &\leq -\eta_1 \langle \nabla L(\theta_1), \theta_2 - \theta_1 \rangle - D_\psi(\theta_2, \theta_0) + D_\psi(\theta^*, \theta_0) \\ &\quad + \eta_1 \langle \tilde{g}_1 - \nabla L(\theta_1), \theta^* - \theta_2 \rangle \\ &\leq \frac{\eta_1^2 K^2}{2\mu} + D_\psi(\theta^*, \theta_0) + \eta_1 \langle \tilde{g}_1 - \nabla L(\theta_1), \theta^* - \theta_2 \rangle. \end{aligned}$$

Then, we conclude that

$$\begin{aligned} \mathbb{E}[L(\hat{\theta}_t) - L(\theta^*)] &\leq \frac{D_\psi(\theta^*, \theta_0)}{H_t} + \frac{K^2}{2\mu} \cdot \frac{\sum_{k=1}^t \eta_k^2}{H_t} \\ &\quad + \frac{R_\Theta C(t)}{m} \cdot \frac{\sqrt{\sum_{k=1}^t \eta_k^2}}{H_t} + (M+1)\sqrt{p}\sigma R_\Theta. \end{aligned}$$

Recall that T is the fixed and known number of iterations. Let $\eta_k = \frac{1}{\sqrt{T}}$ for all $k \geq 1$. Finally we obtain the desired bound as follows:

$$\begin{aligned} \mathbb{E}[L(\hat{\theta}_T) - L(\theta^*)] &\leq \frac{D_\psi(\theta^*, \theta_0)}{\sqrt{T}} + \frac{K^2}{2\mu} \cdot \frac{1}{\sqrt{T}} \\ &\quad + \frac{R_\Theta C(T)}{m} \cdot \frac{1}{\sqrt{T}} + (M+1)\sqrt{p}\sigma R_\Theta. \end{aligned}$$

APPENDIX D PROOF OF LEMMA 3

Proof: The initial lower bound L_1 multiplied by H_1 can be expressed as

$$\begin{aligned} H_1 L_1 &= \eta_1 L(\theta_1) + \eta_1 \langle \tilde{g}_1, \theta_2 - \theta_1 \rangle + \eta_1 \alpha \|\theta_2 - \theta_1\|_2^2 \\ &\quad - \frac{\eta_1 \alpha}{2} \|\theta^* - \theta_1\|_2^2 - \eta_1 \langle \tilde{g}_1 - \nabla L(\theta_1), \theta^* - \theta_1 \rangle. \end{aligned}$$

The corresponding upper bound U_1 multiplied by H_1 can be written as

$$H_1 U_1 = \eta_1 L(\hat{\theta}_1) = \eta_1 L(\theta_1).$$

Then, we have

$$\begin{aligned} H_1 U_1 - H_1 L_1 &= H_1 G_1 \\ &\leq \frac{\eta_1 \alpha}{2} \|\theta^* - \theta_1\|_2^2 + \eta_1 \langle \tilde{g}_1 - \nabla L(\theta_1), \theta^* - \theta_2 \rangle \\ &\quad - \eta_1 \langle \nabla L(\theta_1), \theta_2 - \theta_1 \rangle - \eta_1 \alpha \|\theta_2 - \theta_1\|_2^2 \\ &\leq \frac{\eta_1 \alpha}{2} \|\theta^* - \theta_1\|_2^2 + \eta_1 \langle \tilde{g}_1 - \nabla L(\theta_1), \theta^* - \theta_2 \rangle \\ &\quad + \eta_1 K \|\theta_2 - \theta_1\|_2 - \eta_1 \alpha \|\theta_2 - \theta_1\|_2^2 \\ &\leq \frac{\eta_1 \alpha}{2} \|\theta^* - \theta_1\|_2^2 + \eta_1 \langle \tilde{g}_1 - \nabla L(\theta_1), \theta^* - \theta_2 \rangle + \frac{\eta_1 K^2}{4\alpha} \end{aligned}$$

as desired. \blacksquare

APPENDIX E PROOF OF LEMMA 4

Proof: By the definition of h_t in (11), we have $h_t(\theta_{t+1}) - h_{t-1}(\theta_{t+1}) \geq \eta_t \langle \tilde{g}_t, \theta_{t+1} - \theta_t \rangle + \frac{\eta_t \alpha}{2} \|\theta_{t+1} - \theta_t\|_2^2$. Then, based on the definition of the Bregman divergence, we have

$$\begin{aligned} h_{t-1}(\theta_{t+1}) - h_{t-1}(\theta_t) &= \langle \nabla h_{t-1}(\theta_t), \theta_{t+1} - \theta_t \rangle \\ &\quad + D_{h_{t-1}}(\theta_{t+1}, \theta_t). \end{aligned}$$

Since $\theta_t = \operatorname{argmin}_{u \in \Theta} h_{t-1}(u)$, we have $\langle \nabla h_{t-1}(\theta_t), \theta_{t+1} - \theta_t \rangle \geq 0$. Then:

$$\begin{aligned} h_{t-1}(\theta_{t+1}) - h_{t-1}(\theta_t) &\geq D_{h_{t-1}}(\theta_{t+1}, \theta_t) \\ &= \frac{H_{t-1} \alpha}{2} \|\theta_{t+1} - \theta_t\|_2^2 + \frac{\eta_t \alpha}{2} \|\theta_{t+1} - \theta_t\|_2^2 \\ &\geq \frac{H_{t-1} \alpha}{2} \|\theta_{t+1} - \theta_t\|_2^2. \end{aligned}$$

Hence, we have

$$\begin{aligned} h_t(\theta_{t+1}) - h_{t-1}(\theta_t) &\geq \eta_t \langle \tilde{g}_t, \theta_{t+1} - \theta_t \rangle \\ &\quad + \frac{H_t \alpha}{2} \|\theta_{t+1} - \theta_t\|_2^2 \end{aligned}$$

as desired. \blacksquare

APPENDIX F PROOF OF LEMMA 5

Proof: From Lemma 4, we have

$$\begin{aligned} H_t L_t - H_{t-1} L_{t-1} &\geq \eta_t L(\theta_t) + \eta_t \langle \tilde{g}_t, \theta_{t+1} - \theta_t \rangle + \frac{H_t \alpha}{2} \|\theta_{t+1} - \theta_t\|_2^2 \\ &\quad - \eta_t \langle \tilde{g}_t - \nabla L(\theta_t), \theta^* - \theta_t \rangle \\ &= \eta_t L(\theta_t) + \eta_t \langle \nabla L(\theta_t), \theta_{t+1} - \theta_t \rangle + \frac{H_t \alpha}{2} \|\theta_{t+1} - \theta_t\|_2^2 \\ &\quad - \eta_t \langle \tilde{g}_t - \nabla L(\theta_t), \theta^* - \theta_{t+1} \rangle. \end{aligned}$$

Then, we have

$$\begin{aligned} H_t G_t - H_{t-1} G_{t-1} &\leq H_t L(\hat{\theta}_t) - H_{t-1} L(\hat{\theta}_{t-1}) \\ &\quad - \eta_t L(\theta_t) - \eta_t \langle \nabla L(\theta_t), \theta_{t+1} - \theta_t \rangle - \frac{H_t \alpha}{2} \|\theta_{t+1} - \theta_t\|_2^2 \\ &\quad + \eta_t \langle \tilde{g}_t - \nabla L(\theta_t), \theta^* - \theta_{t+1} \rangle. \quad (19) \end{aligned}$$

Combining the fact that $\hat{\theta}_t = \frac{H_{t-1}}{H_t} \hat{\theta}_{t-1} + \frac{\eta_t}{H_t} \theta_t$ and (16), we have $H_t L(\hat{\theta}_t) - H_{t-1} L(\hat{\theta}_{t-1}) - \eta_t L(\theta_t) \leq 0$. Hence, we may rewrite the right-hand side of (19) as follows

$$\begin{aligned} &- \eta_t \langle \nabla L(\theta_t), \theta_{t+1} - \theta_t \rangle - \frac{H_t \alpha}{2} \|\theta_{t+1} - \theta_t\|_2^2 \\ &\quad + \eta_t \langle \tilde{g}_t - \nabla L(\theta_t), \theta^* - \theta_{t+1} \rangle. \end{aligned}$$

Then, we have

$$\begin{aligned} &- \eta_t \langle \nabla L(\theta_t), \theta_{t+1} - \theta_t \rangle - \frac{H_t \alpha}{2} \|\theta_{t+1} - \theta_t\|_2^2 \\ &\leq \eta_t K \|\theta_{t+1} - \theta_t\|_2 - \frac{H_t \alpha}{2} \|\theta_{t+1} - \theta_t\|_2^2 \\ &\leq \frac{\eta_t^2 K^2}{2H_t \alpha} \leq \frac{\eta_t K^2}{2\alpha}, \quad (20) \end{aligned}$$

where the last inequality from the fact that $H_t \geq \eta_t$.

Combining (19) and (20), we conclude that

$$H_t G_t \leq H_{t-1} G_{t-1} + \eta_t \langle \tilde{g}_t - \nabla L(\theta_t), \theta^* - \theta_{t+1} \rangle + \frac{\eta_t K^2}{2\alpha}$$

as desired. \blacksquare

APPENDIX G PROOF OF COROLLARY 1

Proof: When $\frac{\eta_t}{H_t} = \frac{\alpha}{M}$, we write $G_t = \frac{H_1}{H_t} G_1 + \frac{\sum_{k=2}^t E_k}{H_t}$ as

$$\begin{aligned} G_t &= \frac{H_1}{H_2} \frac{H_2}{H_3} \cdots \frac{H_{t-1}}{H_t} G_1 + \frac{\sum_{k=2}^t E_k}{H_t} \\ &= \left(1 - \frac{\eta_2}{H_2}\right) \left(1 - \frac{\eta_3}{H_3}\right) \cdots \left(1 - \frac{\eta_t}{H_t}\right) G_1 + \frac{\sum_{k=2}^t E_k}{H_t} \\ &= \left(1 - \frac{\alpha}{M}\right)^{t-1} G_1 + \frac{\sum_{k=2}^t E_k}{H_t} \end{aligned}$$

From Lemmas 3 and 5, it follows that

$$\begin{aligned} G_t &= \left(1 - \frac{\alpha}{M}\right)^{t-1} \frac{\alpha}{2} \|\theta^* - \theta_0\|_2^2 + \frac{K^2 \sum_{k=1}^t \eta_k}{2\alpha H_t} \\ &\quad + \frac{\sum_{k=1}^t \eta_k \langle \tilde{g}_k - \nabla L(\theta_k), \theta^* - \theta_{k+1} \rangle}{H_t} \end{aligned}$$

By (18), we obtain the following sequence of upper bounds on the expectation of the final term above:

$$\begin{aligned} &\mathbb{E} \left[\frac{\sum_{k=1}^t \eta_k \langle \tilde{g}_k - \nabla L(\theta_k), \theta^* - \theta_{k+1} \rangle}{H_t} \right] \\ &= \frac{R_\Theta C(t)}{m} \frac{\sqrt{\sum_{k=1}^t \eta_k^2}}{H_t} + (M+1) \sqrt{p\sigma} R_\Theta \\ &= \frac{R_\Theta C(t)}{m} \sqrt{\frac{\sum_{k=1}^t \eta_k^2}{H_t^2}} + (M+1) \sqrt{p\sigma} R_\Theta \\ &= \frac{R_\Theta C(t) \alpha}{mM} \sqrt{\frac{\sum_{k=1}^t H_k^2}{H_t^2}} + (M+1) \sqrt{p\sigma} R_\Theta \\ &= \frac{R_\Theta C(t) \alpha}{mM} \sqrt{\left(\frac{H_1}{H_t}\right)^2 + \cdots + \left(\frac{H_t}{H_t}\right)^2} + (M+1) \sqrt{p\sigma} R_\Theta \\ &\leq \frac{R_\Theta C(t) \alpha}{mM} \sqrt{\frac{1 - (1 - \frac{\alpha}{M})^{2(t-1)}}{1 - (1 - \frac{\alpha}{M})^2}} + (M+1) \sqrt{p\sigma} R_\Theta \\ &\leq \frac{R_\Theta C(t)}{m} + (M+1) \sqrt{p\sigma} R_\Theta. \end{aligned}$$

Therefore, we conclude that:

$$\begin{aligned} \mathbb{E}[L(\hat{\theta}_t) - L(\theta^*)] &\leq \left(1 - \frac{\alpha}{M}\right)^{t-1} \frac{\alpha}{2} \|\theta^* - \theta_0\|_2^2 + \frac{K^2}{2\alpha} \\ &\quad + \frac{R_\Theta C(t)}{m} + (M+1) \sqrt{p\sigma} R_\Theta. \end{aligned}$$

When $\eta_k = \frac{2}{k+1} H_k$, the result of Case 2 follows by substituting this new choice of stepsize into Theorem 2. \blacksquare

APPENDIX H PROOF OF LEMMA 6

Proof: We obtain the following inequality by substituting $C(t) = mt^r$ into the general bound for the smooth and strongly convex case in (12)

$$\begin{aligned} \mathbb{E}[L(\hat{\theta}_t) - L(\theta^*)] &\leq \left(1 - \frac{\alpha}{M}\right)^{t-1} \frac{\alpha}{2} \|\theta^* - \theta_0\|_2^2 + \frac{K^2}{2\alpha} \\ &\quad + R_\Theta t^r + (M+1) \sqrt{p\sigma} R_\Theta. \end{aligned}$$

From the fact that $\|\theta^* - \theta_0\|_2^2 \leq R_\Theta^2$, we can simplify the above upper bound of $\mathbb{E}[L(\hat{\theta}_t) - L(\theta^*)]$ as follows

$$\begin{aligned} \mathbb{E}[L(\hat{\theta}_t) - L(\theta^*)] &\leq \frac{\alpha R_\Theta^2}{2} e^{-\frac{\alpha}{M}(t-1)} + \frac{K^2}{2\alpha} \\ &\quad + R_\Theta t^r + (M+1) \sqrt{p\sigma} R_\Theta. \end{aligned} \quad (21)$$

We take the derivative of the upper bound in (21) with respect to t and set the derivative to be zero as follows:

$$-\frac{\alpha^2 R_\Theta^2}{2M} e^{-\frac{\alpha}{M}(t-1)} + \frac{r \cdot R_\Theta}{t^{1-r}} = 0. \quad (22)$$

Then, we can rewrite (22) as

$$t e^{-\frac{\alpha}{(1-r)M}t} = \left(\frac{2Mr}{\alpha^2 R_\Theta \exp(\alpha/M)} \right)^{\frac{1}{1-r}}.$$

Let $x = -\frac{\alpha}{(1-r)M}t$, we have

$$x e^x = -\frac{\alpha}{(1-r)M} \left(\frac{2Mr}{\alpha^2 R_\Theta \exp(\alpha/M)} \right)^{\frac{1}{1-r}} =: B(r).$$

Therefore, we can obtain the solution t_0 by introducing the Lambert W function W_{-1} as follows:

$$t_0 = \left\lceil -\frac{(1-r)M}{\alpha} W_{-1}(B(r)) \right\rceil.$$

\blacksquare

APPENDIX I PROOF OF THEOREM 3

Proof: Substituting $C(t) = mt^r$ into (12), we obtain

$$\begin{aligned} \mathbb{E}[L(\hat{\theta}_t) - L(\theta^*)] &\leq \left(\prod_{k=2}^t \left(1 - \frac{\eta_k}{H_k}\right) \right) \frac{\alpha}{2} \|\theta^* - \theta_0\|_2^2 + \frac{K^2}{2\alpha} \\ &\quad + R_\Theta t^r \cdot \frac{\sqrt{\sum_{k=1}^t \eta_k^2}}{H_t} + (M+1) \sqrt{p\sigma} R_\Theta. \end{aligned}$$

We now decompose the factor $\prod_{k=2}^t \left(1 - \frac{\eta_k}{H_k}\right)$ as follows:

$$\begin{aligned} \prod_{k=2}^t \left(1 - \frac{\eta_k}{H_k}\right) &= \left(\prod_{k=2}^{t_0} \left(1 - \frac{\alpha}{M}\right) \right) \cdot \prod_{k=t_0+1}^t \left(1 - \frac{2}{k+1}\right) \\ &= \left(1 - \frac{\alpha}{M}\right)^{t_0-1} \cdot \frac{t_0(t_0+1)}{t(t+1)}. \end{aligned}$$

Next, we decompose the term $\frac{1}{H_t} \sqrt{\sum_{k=1}^t \eta_k^2}$ as follows:

$$\frac{\sqrt{\sum_{k=1}^t \eta_k^2}}{H_t} = \sqrt{\sum_{i=1}^{t_0} \left(\frac{\eta_i}{H_t}\right)^2 + \sum_{i=t_0+1}^t \left(\frac{\eta_i}{H_t}\right)^2}. \quad (23)$$

We now seek to bound $\sum_{i=t_0+1}^t (\frac{\eta_i}{H_t})^2$ in (23). We first derive the ratio $(\frac{\eta_{i-1}}{H_t})^2 / (\frac{\eta_i}{H_t})^2$ for all $i \in \{t_0 + 2, \dots, t\}$. Noting that $\frac{\eta_i}{H_i} = \frac{2}{i+1}$,

$$\begin{aligned} \left(\frac{\eta_{i-1}}{H_t}\right)^2 / \left(\frac{\eta_i}{H_t}\right)^2 &= \left(\frac{\eta_{i-1}}{\eta_i}\right)^2 \\ &= \left(\frac{i+1}{i} \cdot \frac{H_{i-1}}{H_i}\right)^2 = \left(\frac{i+1}{i} \cdot \frac{H_i - \eta_i}{H_i}\right)^2 \\ &= \left(\frac{i+1}{i} \cdot \left(1 - \frac{\eta_i}{H_i}\right)\right)^2 = \left(\frac{i+1}{i} \cdot \left(1 - \frac{2}{i+1}\right)\right)^2 \\ &= \left(\frac{i-1}{i}\right)^2. \end{aligned}$$

Hence, we have

$$\begin{aligned} \sum_{i=t_0+1}^t \left(\frac{\eta_i}{H_t}\right)^2 &= \left(\frac{\eta_t}{H_t}\right)^2 \left(1 + \left(\frac{t-1}{t}\right)^2 + \left(\frac{t-2}{t}\right)^2 + \dots + \left(\frac{t_0+1}{t}\right)^2\right) \\ &= \left(\frac{\eta_t}{H_t}\right)^2 \left(\frac{t^2 + (t-1)^2 + (t-2)^2 + \dots + (t_0+1)^2}{t^2}\right) \\ &= \left(\frac{2}{t+1}\right)^2 \left(\frac{\sum_{i=t_0+1}^t i^2}{t^2}\right). \end{aligned} \quad (24)$$

Next, we can bound the remaining part in (23) as follows

$$\begin{aligned} \sum_{i=1}^{t_0} \left(\frac{\eta_i}{H_t}\right)^2 &\stackrel{(a)}{=} \frac{(\frac{\eta_{t_0}}{H_t})^2 (1 - (1 - \alpha/M)^{2t_0})}{1 - (1 - \alpha/M)^2} \\ &\leq \frac{(\frac{\eta_{t_0}}{H_t})^2}{1 - (1 - \alpha/M)^2} \stackrel{(b)}{\leq} \frac{M^2}{\alpha^2} \left(\frac{\eta_{t_0}}{H_t}\right)^2, \end{aligned}$$

where (a) is due to the fact that $(\frac{\eta_j}{H_t})^2 / (\frac{\eta_{j+1}}{H_t})^2 = (1 - \alpha/M)^2$ for all $j \in \{1, \dots, t_0 - 1\}$ and (b) is due to the fact that $1 - (1 - \alpha/M)^2 \geq \alpha^2/M^2$ when $\alpha/M \leq 1$.

To compute $(\frac{\eta_{t_0}}{H_t})^2$, consider

$$\begin{aligned} \frac{\eta_{t_0+1}}{H_{t_0+1}} &= \frac{2}{t_0 + 2}, & \frac{\eta_{t_0+1}}{H_{t_0} + \eta_{t_0+1}} &= \frac{2}{t_0 + 2}, \\ \frac{H_{t_0}}{\eta_{t_0+1}} &= \frac{t_0}{2}, & \frac{\eta_{t_0}}{\eta_{t_0+1}} &= \frac{\alpha}{M} \cdot \frac{t_0}{2}, \end{aligned}$$

where the final equality is because $\eta_{t_0}/H_{t_0} = \alpha/M$.

From $(\frac{\eta_{t_0+1}}{H_t})^2 = (\frac{\eta_t}{H_t})^2 (\frac{t_0+1}{t})^2$, we have the equality $(\frac{\eta_{t_0}}{H_t})^2 = \frac{\alpha^2}{M^2} (\frac{t_0(t_0+1)}{t(t+1)})^2$. Hence,

$$\sum_{i=1}^{t_0} \left(\frac{\eta_i}{H_t}\right)^2 \leq \left(\frac{t_0(t_0+1)}{t(t+1)}\right)^2. \quad (25)$$

By substituting (24) and (25) back into (23), we obtain

$$\frac{\sqrt{\sum_{k=1}^t \eta_k^2}}{H_t} \leq \sqrt{\left(\frac{t_0(t_0+1)}{t(t+1)}\right)^2 + \left(\frac{2}{t(t+1)}\right)^2 \sum_{k=t_0+1}^t k^2}$$

completing the proof upon using the definition of $A(t, t_0)$. ■

REFERENCES

- [1] S. Wang and V. Y. F. Tan, "Robust distributed gradient descent to corruption over noisy channels," in *2024 IEEE International Symposium on Information Theory (ISIT)*. IEEE, 2024, pp. 2520–2525.
- [2] S. Boyd, N. Parikh, E. Chu, B. Peleato, J. Eckstein *et al.*, "Distributed optimization and statistical learning via the alternating direction method of multipliers," *Foundations and Trends® in Machine Learning*, vol. 3, no. 1, pp. 1–122, 2011.
- [3] M. I. Jordan, J. D. Lee, and Y. Yang, "Communication-efficient distributed statistical inference," *Journal of the American Statistical Association*, 2018.
- [4] Y. Low, J. Gonzalez, A. Kyrola, D. Bickson, C. Guestrin, and J. M. Hellerstein, "Distributed graphlab: A framework for machine learning in the cloud," *arXiv preprint arXiv:1204.6078*, 2012.
- [5] P. Richtárik and M. Takáč, "Distributed coordinate descent method for learning with big data," *Journal of Machine Learning Research*, vol. 17, no. 75, pp. 1–25, 2016.
- [6] —, "Parallel coordinate descent methods for big data optimization," *Mathematical Programming*, vol. 156, pp. 433–484, 2016.
- [7] T. Chen, G. Giannakis, T. Sun, and W. Yin, "Lag: Lazily aggregated gradient for communication-efficient distributed learning," *Advances in neural information processing systems*, vol. 31, 2018.
- [8] R. Tandon, Q. Lei, A. G. Dimakis, and N. Karampatziakis, "Gradient coding: Avoiding stragglers in distributed learning," in *International Conference on Machine Learning*. PMLR, 2017, pp. 3368–3376.
- [9] R. Bitar, M. Wootters, and S. El Rouayheb, "Stochastic gradient coding for straggler mitigation in distributed learning," *IEEE Journal on Selected Areas in Information Theory*, vol. 1, no. 1, pp. 277–291, 2020.
- [10] L. Chen, H. Wang, Z. Charles, and D. Papailiopoulos, "DRACO: Byzantine-resilient distributed training via redundant gradients," in *International Conference on Machine Learning*. PMLR, 2018, pp. 903–912.
- [11] Y. Chen, L. Su, and J. Xu, "Distributed statistical machine learning in adversarial settings: Byzantine gradient descent," *Proceedings of the ACM on Measurement and Analysis of Computing Systems*, vol. 1, no. 2, pp. 1–25, 2017.
- [12] D. Yin, Y. Chen, R. Kannan, and P. Bartlett, "Byzantine-robust distributed learning: Towards optimal statistical rates," in *International Conference on Machine Learning*. PMLR, 2018, pp. 5650–5659.
- [13] X. Cao and L. Lai, "Distributed gradient descent algorithm robust to an arbitrary number of byzantine attackers," *IEEE Transactions on Signal Processing*, vol. 67, no. 22, pp. 5850–5864, 2019.
- [14] P. Blanchard, E. M. El Mhamdi, R. Guerraoui, and J. Stainer, "Machine learning with adversaries: Byzantine tolerant gradient descent," *Advances in neural information processing systems*, vol. 30, 2017.
- [15] G. Lan, "An optimal method for stochastic composite optimization," *Mathematical Programming*, vol. 133, no. 1, pp. 365–397, 2012.
- [16] S. Ghadimi and G. Lan, "Optimal stochastic approximation algorithms for strongly convex stochastic composite optimization I: A generic algorithmic framework," *SIAM Journal on Optimization*, vol. 22, no. 4, pp. 1469–1492, 2012.
- [17] O. Devolder, F. Glineur, and Y. Nesterov, "First-order methods of smooth convex optimization with inexact oracle," *Mathematical Programming*, vol. 146, pp. 37–75, 2014.
- [18] M. Cohen, J. Diakonikolas, and L. Orecchia, "On acceleration with noise-corrupted gradients," in *International Conference on Machine Learning*. PMLR, 2018, pp. 1019–1028.
- [19] Q. Zhou and S. J. Pan, "On acceleration for convex composite minimization with noise-corrupted gradients and approximate proximal mapping," *Journal of Machine Learning Research*, vol. 23, no. 223, pp. 1–59, 2022.
- [20] F.-C. Chang, F. Nabiei, P.-Y. Wu, A. Cioba, S. Vakili, and A. Bernacchia, "Gradient descent: Robustness to adversarial corruption," in *OPT 2022: Optimization for Machine Learning (NeurIPS 2022 Workshop)*, 2022.
- [21] C. Hofmeister, L. Maňny, E. Yaakobi, and R. Bitar, "Trading communication for computation in byzantine-resilient gradient coding," in *2023 IEEE International Symposium on Information Theory (ISIT)*. IEEE, 2023, pp. 1985–1990.
- [22] S. Ito, "On optimal robustness to adversarial corruption in online decision problems," *Advances in Neural Information Processing Systems*, vol. 34, pp. 7409–7420, 2021.
- [23] J. Zimmert and Y. Seldin, "An optimal algorithm for stochastic and adversarial bandits," in *The 22nd International Conference on Artificial Intelligence and Statistics*. PMLR, 2019, pp. 467–475.
- [24] Z. Zhong, W. C. Cheung, and V. Tan, "Probabilistic sequential shrinking: A best arm identification algorithm for stochastic bandits with corruptions," in *International Conference on Machine Learning*. PMLR, 2021, pp. 12772–12781.

- [25] S. Sachs, H. Hadji, T. van Erven, and C. Guzmán, “Between stochastic and adversarial online convex optimization: Improved regret bounds via smoothness,” *Advances in Neural Information Processing Systems*, vol. 35, pp. 691–702, 2022.
- [26] D. Bertsekas, A. Nedic, and A. Ozdaglar, *Convex analysis and optimization*. Athena Scientific, 2003, vol. 1.
- [27] Y. Nesterov, “Primal-dual subgradient methods for convex problems,” *Mathematical programming*, vol. 120, no. 1, pp. 221–259, 2009.
- [28] J. Diakonikolas and L. Orecchia, “The approximate duality gap technique: A unified theory of first-order methods,” *SIAM Journal on Optimization*, vol. 29, no. 1, pp. 660–689, 2019.
- [29] A. S. Nemirovskij and D. B. Yudin, *Problem complexity and method efficiency in optimization*. Wiley-Interscience, 1983.
- [30] G. Garrigos and R. M. Gower, “Handbook of convergence theorems for (stochastic) gradient methods,” *arXiv preprint arXiv:2301.11235*, 2023.
- [31] Y. LeCun, L. Bottou, Y. Bengio, and P. Haffner, “Gradient-based learning applied to document recognition,” *Proceedings of the IEEE*, vol. 86, no. 11, pp. 2278–2324, 1998.
- [32] K.-W. Chang, C.-J. Hsieh, and C.-J. Lin, “Coordinate descent method for large-scale l2-loss linear support vector machines,” *Journal of Machine Learning Research*, vol. 9, no. 7, 2008.
- [33] Y. Tang, “Deep learning using linear support vector machines,” *arXiv preprint arXiv:1306.0239*, 2013.
- [34] G. Baruch, M. Baruch, and Y. Goldberg, “A little is enough: Circumventing defenses for distributed learning,” *Advances in Neural Information Processing Systems*, vol. 32, 2019.
- [35] S. Shalev-Shwartz, “Online learning and online convex optimization,” *Foundations and Trends® in Machine Learning*, vol. 4, no. 2, pp. 107–194, 2012.